SCIENCE CHINA
Earth Sciences

SPECIAL TOPIC: Carbon cycling in the China Seas
•REVIEW•

November 2018 Vol.61 No.11: 1564–1582
https://doi.org/10.1007/s11430-017-9267-4

Carbon fluxes in the China Seas: An overview and perspective

Qian LIU, Xianghui GUO, Zhiqiang YIN, Kuanbo ZHOU,
Elliott Gareth ROBERTS & Minhan DAI*

State Key Laboratory for Marine Environmental Science, Xiamen University, Xiamen 361005, China

Received September 14, 2017; revised August 9, 2018; accepted August 31, 2018; published online October 9, 2018

Abstract This paper aims to provide an overview of regional carbon fluxes and budgets in the marginal seas adjacent to China. The "China Seas" includes primarily the South China Sea, East China Sea, Yellow Sea, and the Bohai Sea. Emphasis is given to CO_2 fluxes across the air-sea interface and their controls. The net flux of CO_2 degassing from the China Seas is estimated to be 9.5±53 Tg C yr^{-1}. The total riverine carbon flux through estuaries to the China Seas is estimated as 59.6±6.4 Tg C yr^{-1}. Chinese estuaries annually emit 0.74±0.02 Tg C as CO_2 to the atmosphere. Additionally, there is a very large net carbon influx from the Western Pacific to the China Seas, amounting to ~2.5 Pg C yr^{-1}. As a first-order estimate, the total export flux of particulate organic carbon from the upper ocean of the China Seas is 240±80 Tg C yr^{-1}. This review also attempts to examine current knowledge gaps to promote a better understanding of the carbon cycle in this important region.

Keywords Air-sea CO_2 fluxes, Marine biogeochemistry, Marginal seas, Ocean carbon cycle, China Seas

Citation: Liu Q, Guo X, Yin Z, Zhou K, Roberts E G, Dai M. 2018. Carbon fluxes in the China Seas: An overview and perspective. Science China Earth Sciences, 61: 1564–1582, https://doi.org/10.1007/s11430-017-9267-4

1. Introduction

There has been substantial evidence linking anthropogenic activities to the perturbation of the natural carbon cycle since the industrial revolution (Canadell et al., 2010; Falkowski et al., 2000). In recent history, carbon emissions have increased from 6.4 Pg C yr^{-1} (1 Pg C=10^{15} g C) in the 1990s to 39.2 Pg C yr^{-1} during 2007–2016, including 34.3±2.0 Pg C yr^{-1} released by fossil fuel burning and industrial processes, and 4.9±3.0 Pg C yr^{-1} by land-use change (Le Quéré et al., 2017). About 47% of this anthropogenic CO_2 remains in the atmosphere, while the other 53% enters marine (23%) and terrestrial (30%) ecosystems through air-sea and land-air exchanges (Le Quéré et al., 2017).

By May 2017, the atmospheric CO_2 concentration had reached 406 ppm (https://www.esrl.noaa.gov/gmd/ccgg/trends/global.html) (1 ppm=1 μmol mol^{-1}), an increase of over 45% since the industrial revolution. As a greenhouse gas, increased atmospheric CO_2 concentrations have led to increased surface temperatures on Earth. As such, the study of CO_2 as a key component of the carbon cycle has attracted wide attention, becoming one of the most active research areas in the Earth sciences (Cai et al., 2003; Pan et al., 2011; Regnier et al., 2013; Sabine et al., 2004). These observational studies aim to reduce uncertainties in carbon flux estimates, to clarify anthropogenic perturbations, and to reveal controlling processes and mechanisms in order for a more accurate prediction of future variations in the Earth's climate.

As a gigantic reservoir containing 38118 Pg C (Sarmiento and Gruber, 2002), which far exceeds the amount of carbon stored in the atmosphere, the ocean reduces the rate of increase in atmospheric CO_2. Since the industrial revolution, the ocean has absorbed ~40% of anthropogenic CO_2 (DeVries et al., 2017). Based on the Fifth Assessment Report by the Intergovernmental Panel on Climate Change, the ocean stored 2.0±0.7 Pg C yr^{-1} as anthropogenic CO_2 during 1980–

* Corresponding author (email: mdai@xmu.edu.cn)

1989, and it increased to 2.3±0.7 Pg C yr^{-1} during 2000–2009. This suggests that within this 20 years period, the oceanic carbon storage increased at a rate of 0.15 Pg C every 10 years (Ciais et al., 2013).

The ocean absorbs atmospheric CO_2 primarily through three processes: the "biological pump", the "solubility pump", and the "carbonate pump". The biological pump mainly occurs in the euphotic zone, where phytoplankton transforms dissolved inorganic carbon (DIC) to dissolved organic carbon (DOC) and particulate organic carbon (POC) via photosynthesis. A fraction of this organic carbon is transported into the deep ocean by POC settling and the downward diffusion of DOC. The solubility pump often refers to processes occurring at high latitudes, such as in the North Atlantic Ocean and the Southern Ocean, where seawater cooling and/or freezing promotes an increase in both CO_2 solubility and seawater density that carries high CO_2 water to depth via sinking. The carbonate pump is another important process that exerts a control on the ocean carbon cycle, where carbonate precipitation in seawater leads to the net release of CO_2. A large amount of carbonate in sediments modulates atmospheric CO_2 concentrations through calcium carbonate production and dissolution in the deep sea. Specifically, carbonate dissolution in the deep sea can draw down atmospheric CO_2, while carbonate precipitation can release CO_2 (Elderfield, 2002). Additionally, Jiao et al. (2010) proposed the "non-settling biological pump", or the "microbial carbon pump", which refers to the microbial process of transforming labile DOC to refractory DOC.

For open-ocean CO_2 uptake and release through above processes, large spatial and temporal variations have been observed (Takahashi et al., 2009). The general global trend is that low latitude regimes generally outgas CO_2, and mid- and high latitude regions often absorb CO_2. In particular, the North Atlantic Ocean and the Southern Ocean are two of the strongest sinks for anthropogenic CO_2. Regions where mode water is produced in mid-latitude are also important sinks of atmospheric CO_2. In contrast, the equatorial Pacific Ocean is a very big carbon source with the highest inter-annual variability (Takahashi et al., 2009 and references therein).

Marginal seas have their own unique geographical, physical, chemical, and biological characteristics that include intensive land-ocean-atmosphere interactions (Dai et al., 2013a). Firstly, marginal seas are significantly affected by terrestrially-sourced natural and anthropogenic carbon and nutrients (Liu et al., 2010a). Secondly, they generally have high rates of primary productivity, as well as a complicated biological community structure (Liu et al., 2010a, 2010b). The primary production, microorganism recycling, and carbon settling and export that occur in marginal seas vary with respect to these same processes in the open ocean. Thirdly, at marginal seas with relatively shallow water depths, particulate carbon can quickly settle to the bottom and affect the sediment-water interface (Hung et al., 2013), and therefore can directly influence the carbon cycle in the overlying seawater and CO_2 exchange at the air-sea interface. Lastly, the CO_2 absorbed by marginal seas can be exported to the open ocean via the continental shelf pump (Tsunogai et al., 1999) and vice-versa (e.g., Dai et al., 2013a and references therein). Additionally, coastal upwelling complicates the role of the ocean margin as a CO_2 sink or source by bringing CO_2 and nutrient-enriched deep water to the surface. If the increase in primary productivity stimulated by the additional nutrients cannot compensate the free CO_2 brought up from depth, the coastal system will tend to release CO_2 to the atmosphere (Cai, 2011).

Over the past two decades, significant research efforts have been devoted to the study of the carbon cycle in marginal seas. Considerable field observations and simulations were conducted that have significantly improved the accuracy of air-sea CO_2 flux estimates therein, as well as our understanding of ocean margin carbon cycling as a whole. Previous synthesis analyses of available data revealed that marginal seas appear to be a sink of atmospheric CO_2 on a global scale, of approximately 0.2–0.4 Pg C yr^{-1} (Borges, 2011; Borges et al., 2005; Cai, 2011; Cai et al., 2006; Chen and Borges, 2009; Dai et al., 2013a; Laruelle et al., 2010; Liu et al., 2010a). Laruelle et al. (2014) updated this estimation by considering the partial sea ice cover of polar shelves by utilizing the global ocean CO_2 atlas (Surface Ocean CO_2 Atlas, SOCAT) data. This led to a new approximation of atmospheric CO_2 uptake by marginal seas of 0.19±0.05 Pg C yr^{-1}, which is the lower boundary of the previous estimates.

It was previously postulated that the latitude of an ocean margin determined its CO_2 sink-source pattern (Cai and Dai, 2004; Cai et al., 2006). Owing to high temperatures and large inputs of terrestrial organic carbon, low latitude marginal seas typically release CO_2 (Cai and Dai, 2004; Cai et al., 2006; Cai, 2011). Assessments of global riverine DOC fluxes revealed that 60% of the riverine DOC are discharged into low-latitude seas (Dai et al., 2012). Dai et al. (2013a) proposed that world marginal seas, in terms of external carbon inputs and internal cycling rates, can be placed into at least two categories: river-dominated ocean margins (RiOMars) and ocean-dominated margins (OceMars). RiOMars are featured by concurrent inputs of high loadings of both autotrophic (nutrients) and heterotrophic (organic matter) material, while OceMars are characterized by concurrent offsite sources, along the barocline, contributing nutrients and dissolved inorganic carbon (DIC) into the system (Dai et al., 2013a; Cao et al., 2014).

This study sought to synthesize CO_2 air-sea fluxes of the marginal seas adjacent to China (China Seas): the South China Sea (SCS), East China Sea (ECS), Yellow Sea (YS) and Bohai Sea (BS) (Figure 1). We summarized carbon

fluxes along the river-sea interface, carbon exchange between the ocean margin and the open ocean, and POC export fluxes from the euphotic layer. Based on this analysis, we constructed a preliminary and simplified carbon budget for the China Seas and compared our estimates with air-sea CO_2 fluxes in other marginal seas worldwide.

2. The carbon cycle in the China Seas

The China Seas account for approximately 12% of the total surface area of global continental margins, and span the temperate, subtropical, and tropical zones. The China Seas receive inputs from large rivers such as the Changjiang (Yangtze) and Zhujiang (Pearl) rivers, and also exchange with the Kuroshio, a major western ocean boundary current. As a result, the carbon cycle in the China Seas is rather complex (Dai et al., 2004), and have attracted great attention in the past few decades. At the beginning of this century, Chinese scientists published a first monograph on material fluxes on continental margins (Hu and Yang, 2001), in which the ECS was revealed as a weak sink for atmospheric CO_2. This result, as well as multiple studies on the CO_2 sink-source pattern in the ECS conducted by scientists from surrounding countries and regions (Chou et al., 2009, 2011; Shim et al., 2007; Tsunogai et al., 1999), have been widely discussed in international communities. The ECS has therefore been frequently cited as a case-study of global continental margins that absorb atmospheric CO_2. More recently, the Ministry of Science and Technology of China, the Natural Science Foundation of China, the State Oceanic Administration (SOA), and the Chinese Academy of Sciences have funded a number of projects related to carbon cycle to investigate material transport, nutrient cycling, and primary productivity in the China Seas. These financial contributions enabled scientists to obtain a large amount of observational data and results. Major projects, such as the "Carbon Cycle in the South China Sea: budget, controls & global implications" under the National Key Basic Research Program of China, are still ongoing to better understand the ocean's carbon cycle in the China Seas (Dai and Yin, 2016).

2.1 Air-sea CO_2 fluxes

2.1.1 South China Sea

Based on a mass balance model built on a limited dataset collected in the 1990s, Chen et al. (2006) concluded that the SCS basin is a weak source of atmospheric CO_2. However, time-series observational studies at SEATS (The South East Asia Time-series Station, Figure 1) in the northern SCS

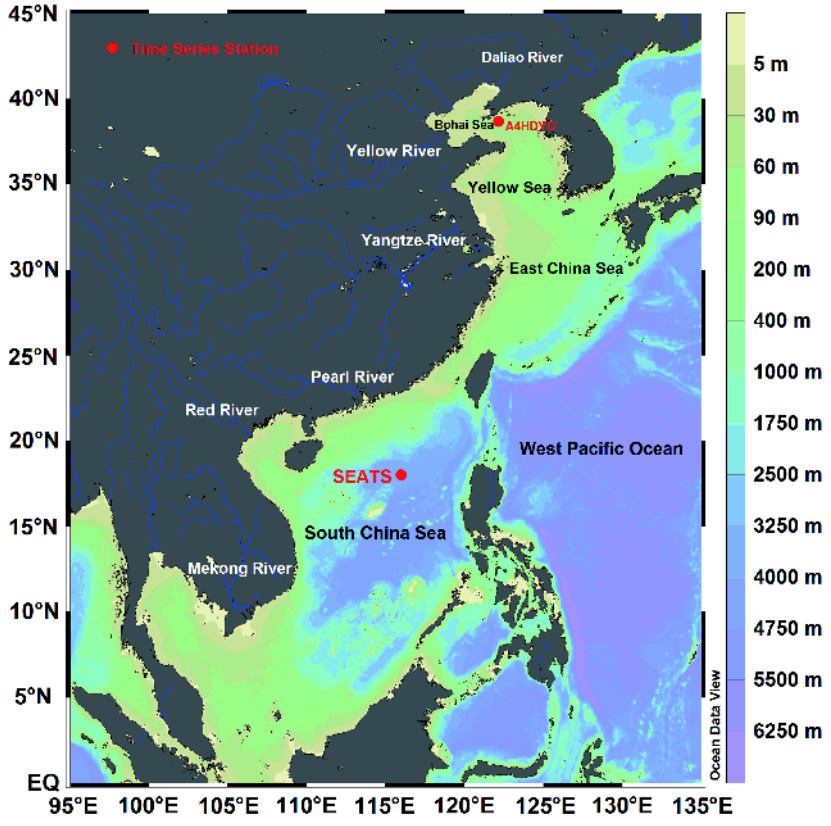

Figure 1 Geographic map of the China Seas. SEATS (South East Asian Time-Series Study) represents the time-series station in the South China Sea (Chou et al., 2005), and A4HDYD represents the time-series station in the Yellow Sea (Xu et al., 2016).

(NSCS) basin showed that the region is a weak CO_2 sink or near equilibrium with the atmosphere on an annual basis between December 1999 and December 2009 (Chou et al., 2005; Sheu et al., 2010; Tseng et al., 2007). Other field surveys show that the NSCS, including the shelf region, is a CO_2 source during warm seasons, a CO_2 sink during cold seasons, and a weak source on an annual scale (Zhai et al., 2005, 2009). The Sunda shelf in the southern SCS is also a CO_2 source in early fall (Rehder and Suess, 2001).

Zhai et al. (2013) provided the most comprehensive assessment of CO_2 fluxes and their controls in the SCS, based on a large dataset of 14 field CO_2 mapping surveys between 2003 and 2008. These authors divided the SCS into 4 domains, according to zonal physical and biogeochemical characteristics (Figure 1 in Zhai et al., 2013). In their study, Domain A was the NSCS shelf influenced by the Zhujiang River, Domain B was the NSCS slope and basin, Domain C was the middle SCS basin, and Domain D was the basin west of the Luzon Strait, which might be affected by winter upwelling. The partial pressure of CO_2 (pCO_2) in Domain A was relatively low and showed little seasonal variation (320–390 μatm). pCO_2 in Domain B revealed a seasonal pattern of high values during warm seasons (summer and spring) and low values during cold seasons (winter and fall). pCO_2 in Domain C was relatively high all year round (360–425 μatm). In Domain D, pCO_2 was high during the winter upwelling periods. The area-weighted annual average CO_2 flux was 1.1±1.7 mmol m^{-2} yr^{-1}, and the 4 domains emitted 18±27.6 Tg C yr^{-1} of CO_2 (with the surface area of the 4 domains being 1.34×10^6 km^2). Extrapolated to the entire SCS proper (with a surface area of 2.5×10^6 km^2 excluding the Gulfs of Thai and Beibu), the entire SCS emitted 33.6±51.3 Tg C yr^{-1} (1 Tg C=10^{12} g C; Zhai et al., 2013).

The major controls of surface water pCO_2 and air-sea CO_2 fluxes differ among the 4 domains. pCO_2 in Domain A is mainly driven by biological processes and seasonal variations in sea surface temperature (SST), whereby pCO_2 is drawn down due to cooling during cold seasons and high rates of phytoplankton uptake during warm seasons (i.e. summer). pCO_2 in Domain B is mainly controlled by SST, with low pCO_2 during cold seasons and high pCO_2 during warm seasons. pCO_2 in Domain C is also dominated by temperature, where high temperatures during all the seasons results in high pCO_2 values throughout the year. Air-sea CO_2 fluxes in Domain D are mainly dominated by winter upwelling (Zhai et al., 2013).

2.1.2 *East China Sea*

The CO_2 in ECS surface water is usually undersaturated with respect to the atmosphere, and thus the ECS generally serves as an annual net sink of atmospheric CO_2 with an air-sea CO_2 flux in the range of –(10–30) Tg C yr^{-1} (Chou et al., 2009, 2011, 2013; Peng et al., 1999; Shim et al., 2007; Tsunogai et al., 1999; Wang et al., 2000; Tseng et al., 2011). Based on a dataset from 8 summer cruises and 5 cruises conducted during other seasons, Tseng et al. (2014) evaluated the annual average air-sea CO_2 flux to be −1.8±0.5 mol C m^{-2} yr^{-1} by establishing an empirical formula between surface water pCO_2 and freshwater discharge from the Changjiang River. It should be noted that high pCO_2 in fall is a typical feature in the ECS, which has been often observed (Zhai and Dai, 2009; Zhai et al., 2007), but it is not a function of Changjiang discharge (e.g., Zhai and Dai, 2009), therefore the empirical algorithm cannot accurately estimate the distributions of surface water pCO_2 in fall.

Based on 24 surveys conducted over the entire ECS shelf in 4 seasons of the year during 2006–2011, Guo et al. (2015) presented a comprehensive dataset of surface seawater pCO_2 and associated air-sea CO_2 fluxes. They classified the ECS into 5 domains that featured differing physics and biogeochemistry (Figure 1 in Guo et al., 2015). The 5 domains were the Changjiang plume (I), the Zhejiang-Fujian coast (II), the northern shelf (III), the middle shelf (IV), and the southern shelf (V). Overall, surface water pCO_2 showed strong spatial and seasonal variations. In the Changjiang plume, pCO_2 was as low as <100 μatm during winter, spring, and summer, but high in the fall (>360 μatm). Along the Zhejiang-Fujian coast, pCO_2 during winter, spring, and summer (300–350 μatm) were also lower than during fall (>350 μatm), but the seasonal variation was smaller than the Changjiang plume seasonal variability. In the ECS outer shelf (the area impacted by the Kuroshio), pCO_2 was higher during warm seasons than cold seasons (Figure 2).

In general, the Changjiang plume and the Zhejiang-Fujian coast were sinks of atmospheric CO_2 during winter, spring and summer, but a CO_2 source in fall. The northern, middle, and southern shelves were sinks of atmospheric CO_2 during cold seasons and CO_2 sources during warm seasons. Overall, the 5 domains were all CO_2 sinks annually with an area-weighted CO_2 flux of −2.5±1.5 mol m^{-2} yr^{-1} (Guo et al., 2015). This approximation was twice the global average of marginal seas CO_2 fluxes. The surface area of the ECS with water depths <200 m is 0.45×10^6 km^2, and this region absorbed CO_2 from the atmosphere at a rate of 13.2 Tg C yr^{-1} (Guo et al., 2015). Extrapolated to the entire ECS (0.77×10^6 km^2), it sequesters 23.3±13.5 Tg C yr^{-1} of CO_2.

The major controls on air-sea CO_2 fluxes differ in the 5 domains of the ECS. Surface water pCO_2 in the Changjiang plume and the Zhejiang-Fujian coast are mainly controlled by SST, biological processes, and vertical mixing. pCO_2 is low in winter due to low SST in domains I and II. During warm seasons, the water column is stratified and biological uptake decreases the surface water pCO_2. In fall, the stratification is destroyed by the decrease in SST and strong winds and surface pCO_2 increases due to enhanced vertical mixing of the CO_2-enriched bottom/subsurface water. However,

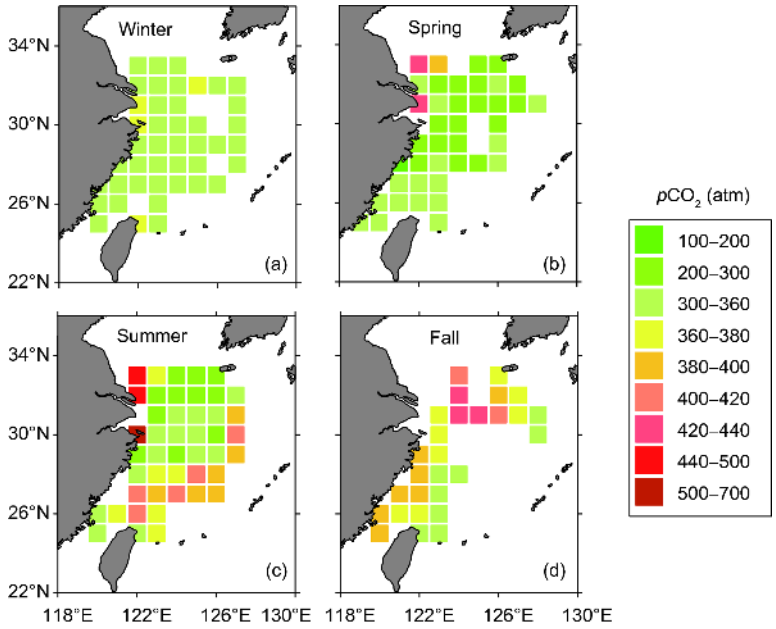

Figure 2 Distribution of seasonal averages of pCO_2 in 1°×1° grids on the East China Sea (ECS) shelf (based from Guo et al., 2015). Atmospheric CO_2 increased at a rate of 2 μatm yr^{-1} (http://scrippsco2.ucsd.edu/), leading to a similar rate of increase in sea surface pCO_2. Tseng et al. (2014) report that pCO_2 in the surface water of the ECS increases at a rate of 2.1 μatm yr^{-1}. Since the sea surface pCO_2 data used in this study was collected from different cruises during 2006 to 2011, the seawater pCO_2 data were normalized to June 2010 at the rate of 2.1 μtm yr^{-1}. When estimating the gridded average, the pCO_2 data from each cruise was first constrained to the 1°×1° grid, and then the average value during each season was calculated.

pCO_2 in the domains III, IV, and V is dominated by SST; i.e. containing low pCO_2 with respect to the atmosphere during cold seasons and higher pCO_2 in warm seasons (Guo et al., 2015).

In summary, various domains are very different with respect to air-sea CO_2 fluxes and major controls on surface water pCO_2. Within the domains I and II, pCO_2 is low during winter, spring and summer, but high in the fall. For example, in the domain I, the seasonal average pCO_2 during winter, spring, summer, and fall were 348, 309, 317, and 394 μatm, and the air-sea CO_2 fluxes were −9.8, −10.7, −6.5, and 2.2 mmol m^{-2} d^{-1}, respectively within the investigation by Guo et al. (2015). Therefore, the domain I is a CO_2 sink in winter, spring, and summer, and a CO_2 source during the fall. However, the outer shelf is temperature dominated; its seasonal average pCO_2 and air-sea CO_2 fluxes during the 4 seasons at the investigation's time-frame were 344, 345, 381, and 348 μatm, and −10.0, −6.8, 1.8, and −8.4 mmol m^{-2} d^{-1}, respectively. Thus, the outer shelf is a CO_2 sink in winter, spring and fall, but a CO_2 source in the summer.

2.1.3 *Yellow Sea*

The YS is geographically divided into the North Yellow Sea (NYS) and the South Yellow Sea (SYS, along a line between Cape Chengshan on the Shandong Peninsula in China and Changshanchuan on the Korea Peninsula). Surface water pCO_2 in the YS in April 1996 was 220–360 μatm, with an average CO_2 flux of −2.34 mol m^{-2} yr^{-1}. This estimation indicated that the YS is a moderate sink of atmospheric CO_2 (Oh et al., 2000). During 2006–2007, Xue et al. (2012) conducted 4 surveys in the YS and revealed that it is a CO_2 source during all seasons, and it was a weak source on an annual scale (0.63±0.10 mol m^{-2} yr^{-1} of CO_2). Based on time-series observations during the period of March 2011 to November 2013 at station A4HDYD located in the northwest of the NYS (Figure 1), the NYS is a weak sink of atmospheric CO_2 (−0.85±0.59 mol C m^{-2} yr^{-1}, Xu et al., 2016). In summation, CO_2 in the NYS is generally near equilibrium with the atmosphere.

In the SYS, with data from observations during spring, summer, and fall, Xue et al. (2011) estimated the annual average air-sea CO_2 flux to be 1.32 mol m^{-2} yr^{-1}. This result indicated that the SYS is a weak source of atmospheric CO_2. However, Qu et al. (2014) found that the western and central regions of the SYS were a weak CO_2 sink (−1.02 mol m^{-2} yr^{-1}). Similarly, Luo et al. (2015) argued that the central YS is a weak CO_2 sink (−0.70 mol m^{-2} yr^{-1}) based on estimations using numerical models.

SOA surveyed the entire YS and found that it was a sink of atmospheric CO_2 during winter, spring, and summer, but a source in the fall. Annually, the YS was estimated to be a weak CO_2 sink (−0.2±0.1 mol m^{-2} yr^{-1}, State Oceanic Administration, 2013). The YS sequesters 1.0±0.3 Tg C yr^{-1} of CO_2 if a surface area of 0.38×10^6 km^2 is adopted (State Oceanic Administration, 2013).

2.1.4 *Bohai Sea*

Generally, the study of air-sea CO_2 fluxes in the BS has been

very limited. The CO_2 flux was found to be 1.01 mol m^{-2} yr^{-1} in September, 2009 (Yin et al., 2012). Surveys conducted by the SOA (2013) during 2011–2012 show that the BS is a source of atmospheric CO_2 in fall, a sink in winter and spring, and near-equilibrium with the atmosphere in summer. Annually, the BS is a weak source (0.2±0.1 mol m^{-2} yr^{-1}) and emitting 0.2±0.1 Tg C yr^{-1} of CO_2 to the atmosphere if a surface area of 7.7×10^4 km^2 is adopted (SOA, 2013).

To sum up, the SCS is a CO_2 source (33.6±51.3 Tg C yr^{-1}), the ECS is a CO_2 sink (23.3±13.5 Tg C yr^{-1}), and the YS (1.0±0.3 Tg C yr^{-1}) and BS (0.2±0.1 Tg C yr^{-1}) are in near-equilibrium with the atmosphere with respect to CO_2 (Figure 3). The China Seas, as a whole, are a source of atmospheric CO_2 and emit 9.5±53 Tg C yr^{-1} of CO_2 (Figure 3).

2.2 Lateral transport of carbon from land to the ocean

Rivers and estuaries are often overlooked in regional carbon cycle budgets because of their small size. However, they are an important material pathway from land to the ocean. Fixed carbon in soils enters rivers and estuaries via soil weathering and erosion. During transport from rivers/estuaries to marginal seas, a portion of the carbon is emitted to the atmosphere as CO_2. A part of this carbon is transformed into different carbon pools by complex biogeochemical processes within the estuaries. Then, a minor fraction is buried in the sediments of rivers and estuaries, with the remaining carbon exported to the marginal seas. Regnier et al. (2013) estimated the global carbon budget under anthropogenic perturbations. They suggested that since the industrial revolution, ~1.0 Pg C yr^{-1} of anthropogenic carbon was delivered from soils to inland waters (mainly rivers), with approximately 40% of the carbon outgassed to the atmosphere (0.4 Pg C yr^{-1}), 50% of the carbon sequestered by river, estuarine, and coastal sediments, and the remaining 10% discharged into the ocean (0.1 Pg C yr^{-1}).

There are four major rivers discharging into the China Seas: the Mekong River, the Zhujiang River, the Changjiang River and the Huanghe (Yellow) River. The Changjiang River is the largest river in China and the third largest river in the world, with a discharge rate (~900 km^3 yr^{-1}) accounting for 56% of the total river flow (1600 km^3 yr^{-1}) in China (Dai, 2016). The Changjiang River transports substantial amounts of freshwater, carbon, and nutrients to the ECS and YS. The Zhujiang River is the second largest river in China in terms of freshwater discharge (275 km^3 yr^{-1}, Huang et al., 2017), and significantly impacts the northeast SCS shelf. The Mekong River is the seventh largest river worldwide (474 km^3 yr^{-1}, Huang et al., 2017), discharging into the SCS from Vietnam. The Huanghe River carries the largest amount of suspended particulates of the four rivers and discharges into the BS in the Shandong province (Dai et al., 2013a).

2.2.1 *Fluvial total carbon fluxes to the China Seas*

To evaluate the total riverine carbon fluxes to the China Seas, we first calculated river discharge-weighted average carbon concentrations using known forms of oceanic carbon (DIC, DOC, POC, and Particulate Inorganic Carbon, PIC) concentrations of several rivers and their corresponding freshwater discharge. The total riverine carbon flux into the estuaries was calculated as the product of discharge-weighted average carbon concentrations and total freshwater discharge into the China Seas. The estuary is not only a passageway of materials from land to the ocean, but also a "reactor". Biogeochemical processes lead to the addition or removal of carbon within the estuary and modify the net carbon flux to the sea. Therefore, the total riverine carbon flux into the China Seas was calculated by applying esti-

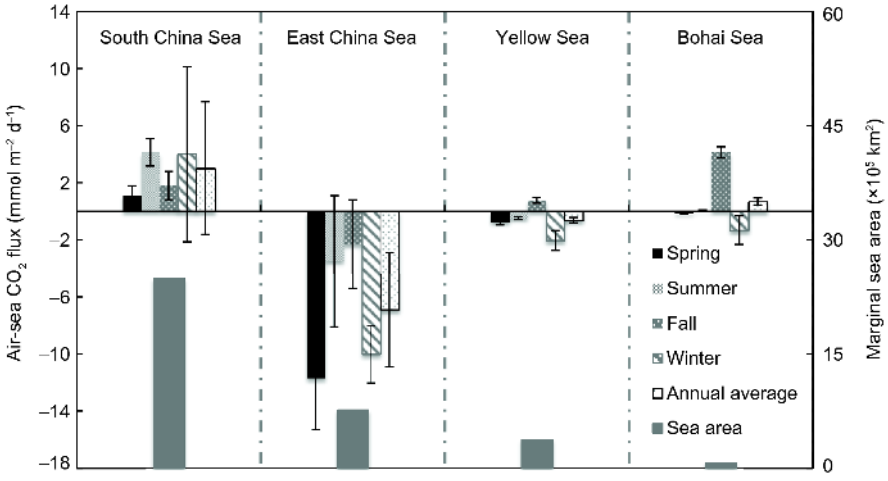

Figure 3 Air-sea CO_2 seasonal variations and annual fluxes in the China Seas (South China Sea, East China Sea, Yellow Sea, and Bohai Sea). Negative values denote seawater absorbing CO_2 from the atmosphere. Sea surface pCO_2 values in the South China Sea and East China Sea were derived from Zhai et al. (2013) and Guo et al. (2015), respectively. pCO_2 data in the Yellow Sea and Bohai Sea were primarily obtained from the State Oceanic Administration (2013). For air-sea CO_2 fluxes, the average values are shown. The error bars represent standard deviation, which characterizes the spatial variations in fluxes. Details are presented in the text.

mates of removal/addition rates of carbon in the estuaries to the riverine inputs. It should be noted that the Mekong River and the Zhujiang River are the two largest rivers flowing into the SCS. In addition, several other rivers located in south China, Vietnam, the Philippines, and Malaysia also discharge into the SCS, and are included in our calculations (Table 1).

(1) Changjiang River and Changjiang estuary. There are no marked seasonal variations of DIC and DOC in the Changjiang River. DIC ranged from 1585–1978 μmol kg^{-1} (Zhai et al., 2007), with an average concentration of 1746±159 μmol kg^{-1}. DOC concentrations fluctuated from 1.64–2.74 mg L^{-1} (Wang et al., 2012), with a mean value of 2.03±0.27 mg L^{-1}. The POC/DOC ratio is approximately 1 (Wang et al., 2012; Wu et al., 2007), comparable to the global mean ratio (McKee, 2003). POC and PIC show strong seasonal variations and are higher during summer than in winter. POC and PIC ranged from 0.58–3.60 mg L^{-1} (mean 1.67±0.94 mg L^{-1}) and 0.17–0.70 mg L^{-1} (0.36±0.16 mg L^{-1}) (Wang et al., 2012), respectively. The DIC, DOC, PIC, and POC fluxes from the Changjiang River to the Changjiang estuary were 19.0±1.7, 1.84±0.2, 0.34±0.2, and 1.51±0.8 Tg C yr^{-1}. These fluxes were calculated as the average concentrations of carbon (DIC, DOC, PIC, and POC) multiplied by mean Changjiang River discharge (from 1900–2004; Dai, 2016). Subsequently, the total carbon flux discharge into the Changjiang estuary was 22.7±1.9 Tg C yr^{-1}.

(2) Zhujiang River and Zhujiang River estuary. The concentration of DIC at the freshwater end-member in the Zhujiang River estuary is higher during winter (>2700 μmol kg^{-1}) than in summer (1000 μmol kg^{-1}), with an average of 1740 μmol kg^{-1} (Guo et al., 2008). DOC concentrations ranged from 1.38–2.13 mg L^{-1}, with a mean of 1.67 mg L^{-1} from 8 major riverine runoff outlets in the Zhujiang River (Ni et al., 2008). The DOC concentration during the dry season is higher than during the wet season, although this pattern is reversed for POC. Therefore, the POC/DOC ratio is higher during the wet season relative to the dry season (1–4 vs 0.2–1). PIC data is not available from the Zhujiang River estuary, if PIC is assumed to account for 0.97% of the total suspended matter (TSM; Huang et al., 2017), PIC concentrations would be 1.59 mg L^{-1}. Using a similar approach for calculating Changjiang River carbon fluxes, we estimate the DIC, DOC, PIC, and POC fluxes to the Zhujiang River estuary as 5.75±3.3, 0.46±0.3, 0.44±0.3 and 2.10±1.2 Tg C yr^{-1}, respectively. The total carbon input flux is estimated as 8.75±3.5 Tg C yr^{-1}.

(3) Huanghe River and Yellow River estuary. The DIC concentration in the Huanghe River during the dry season (2570–3640 μmol kg^{-1}) is higher than in the wet season (2269–2752 μmol kg^{-1}), with an average of 3197 μmol L^{-1} (Zhang and Zhang, 2007; Ran et al., 2013). The monthly variability in DOC (Lijin gauge station) was small, which ranges from 1.81–3.36 mg L^{-1} (Wang et al., 2012) to 2.83–3.85 mg L^{-1} (Ran et al., 2013), with an average value of 2.83±0.56 mg L^{-1}. Unlike in the Changjiang River and Zhujiang River, the POC/DOC ratio in the Huanghe River is as high as 12 (Wang et al., 2012). POC displayed large monthly variations with an average value of 14.6±14.3 mg L^{-1}. The annual DIC, DOC, PIC, and POC flux discharge into the Yellow River estuary were 1.46±0.3, 0.11±0.02, 2.35±3.5 and 0.56±0.7 Tg C yr^{-1}, with a total carbon flux of 4.47±3.6 Tg C yr^{-1}.

To summarize, the annual fluxes of DIC, DOC, PIC, and POC from the three major Chinese rivers to their estuaries were 26.2±3.7, 2.67±0.4, 3.11±3.5 and 4.17±1.6 Tg C yr^{-1}, with a total carbon flux of 36.2±5.3 Tg C yr^{-1}.

(4) Total riverine carbon flux discharging into the estuaries. Recently, Huang et al. (2017) compiled a dataset of riverine fluxes and carbon concentrations from 51 rivers around the SCS, including the Mekong and the Zhujiang River. Xia and Zhang (2011) reported the concentrations of DIC, DOC, and POC in 16 rivers that discharge into the BS, such as the Ziyaxin River and the Daliaohe River. We calculated the river discharge-weighted average carbon concentrations as follows: we sum the products that were obtained for each river by multiplying discharge and their corresponding carbon concentrations, and then divide by the total discharge of the rivers (only rivers with known carbon concentrations were included). Using the calculated discharge-weighted average carbon concentration and total reported river discharge into the China Seas (2208 km^3 yr^{-1}, including 34 rivers in China, and 13 rivers discharging into the SCS from the Philippines, Vietnam and Malaysia), we estimated the total riverine carbon flux discharging into the estuaries to be 64.9±6.8 Tg C yr^{-1}, of which, 40.8±4.8 Tg C yr^{-1} was DIC, 6.87±1.3 Tg C yr^{-1} was DOC, 4.05±3.7 Tg C yr^{-1} was PIC, and 13.3±2.8 Tg C yr^{-1} was POC. Here, we do not consider the rivers those flow into the Gulf of Thailand. River discharge, carbon concentrations, and carbon fluxes are shown in Table 1.

(5) Total riverine carbon flux discharging into the China Seas. To calculate the riverine carbon flux into marginal seas, the addition or removal of carbon in estuaries needs to be considered. For example, biogeochemical processes at the southern branch and the northern branch of the Changjiang estuary differ significantly. The southern branch acts like a "channel" through which terrestrial material enters the sea. In contrast, the northern branch behaves more like a "reactor", where strong organic carbon mineralization and DIC regeneration exist (Zhai et al., 2017). Zhai et al. (2017) found that the DIC released by biogeochemical processes (organic carbon mineralization and $CaCO_3$ dissolution) in the northern branch of the Changjiang estuary accounts for 1.5–6.9% of the total DIC flux discharged from the Changjiang River in April 2010. These findings are distinct from findings in the Zhujiang estuary, where summer phytoplankton blooms at

Table 1 Riverine carbon concentrations and fluxes into the China Seas[a)]

River	River flow (km^3 yr^{-1})	Carbon concentration[$]				Carbon flux (Tg C yr^{-1})				
		DIC	DOC	PIC	POC	DIC	DOC	PIC	POC	Total C flux
Changjiang[#]	908	1746	2.03	0.36	1.67	19.0±1.7	1.84±0.2	0.34±0.2	1.51±0.8	22.7±1.9
Zhujiang River[%]	275	1740	1.67	1.59	7.62	5.75±3.3	0.46±0.3	0.44±0.3	2.10±1.2	8.75±3.5
Huanghe River[#]	38	3197	2.83	61.6	14.6	1.46 ±0.3	0.11±0.02	2.35±3.5	0.56±0.7	4.47±3.6
Mekong[%]	474	1026	4.48	0.35	8.31	5.84	2.12	0.16	3.94	12.06
Liaohe/Shuangtaizihe[&]	13	2645	5.88	-	9.25	0.42	0.08	-	0.12	-
Daliaohe[&]	20	2338	4.71	-	4.95	0.55	0.09	-	0.1	-
Dalinghe[&]	0	2814	3.83	-	16.5	0.01	0	-	0.01	-
Xiaolinghe[&]	15	3349	5.07	-	6.9	0.61	0.08	-	0.1	-
Liuguhe[&]	3	1601	2.58	-	3.04	0.05	0.01	-	0.01	-
Luanhe[&]	8	3896	2.58	-	9.81	0.37	0.02	-	0.08	-
Ziyaxinhe[&]	22	5948	30.7	-	11.8	1.56	0.67	-	0.26	-
Tuhaihe[&]	2	2866	4.57	-	9.12	0.08	0.01	-	0.02	-
Choshui[%]	10	2697	1.42	4.53	33.7	0.33	0.01	0.05	0.34	0.73
Hanjiang[%]	16	663	1.26	2.83	8.48	0.13	0.02	0.05	0.14	0.33
Jian Jiang[%]	5	462	2.33	3.04	4.58	0.03	0.01	0.01	0.02	0.07
Jiulong Jiang[%]	8	536	1.84	10.2	41.1	0.05	0.01	0.08	0.33	0.47
Kaoping[%]	3	2308	0.79	-	-	0.08	0	-	-	-
Lawis[%]	16	1765	0.5	11.2	81.3	0.33	0.01	0.17	1.26	1.78
Canal[%]	8	500	4.75	3.88	55.6	0.05	0.04	0.03	0.46	0.58
Moyang Jiang[%]	10	634	1.43	5.97	40.5	0.08	0.01	0.06	0.4	0.55
Nanliu Jiang[%]	2	194	1.91	7.36	54.5	0.01	0	0.02	0.12	0.14
Pampanga[%]	4	2826	5.76	6.25	64.2	0.15	0.03	0.03	0.29	0.49
Qin Jiang[%]	2	344	1.96	0.67	2.58	0.01	0	0	0	0.02
Rong Jiang[%]	2	1089	3.37	-	-	0.03	0.01	-	-	-
Saigon[%]	36	749	2.15	-	-	0.33	0.08	-	-	-
Song Hau[%]	21	835	2.36	-	-	0.21	0.05	-	-	-
Tsengwen[%]	2	3307	3.48	1.06	5.83	0.07	0.01	0	0.01	0.08
Yong Jiang[%]	5	2305	1.18	2.52	11.7	0.14	0.01	0.01	0.06	0.22
Rajang[%]	150	360	2.80	1.19	1.63	0.65	0.42	0.03	0.24	1.34
All rivers[*]	2208	1539	3.11	1.83	6.00	40.8±4.8	6.87±1.3	4.05±3.7	13.3±2.8	64.9±6.8
Riverine C into the China Seas	2208	1539	2.80	1.83	3.90	40.8±4.8	6.19±1.1	4.05±3.7	8.62±1.8	59.6±6.4

a) [$]DIC values are reported in μmol L^{-1}. DOC, PIC, and POC are reported in mg L^{-1}. [#]River flow values are from Dai (2016); carbon concentrations in the Changjiang River are from Wang et al. (2012) and Zhai et al. (2007); carbon concentrations in the Huanghe River are from Wang et al. (2012), Ran et al. (2013), Zhang and Zhang (2007). [%]River flow and carbon concentrations are derived from Huang et al. (2017) and references therein. [&]River flow data are downloaded from the Hydrology Bureau of Ministry of Water Resources (http://xxfb.hydroinfo.gov.cn/); carbon concentrations are from Xia and Zhang (2011). [*]Total river flow includes 47 rivers that discharge into the China Seas. In addition to the rivers showed in this table, we took into account the Huaihe[#], Oujiang[#], Jiyunhe[#], Yanghe[&], Fuzhouhe[&], Biliuhe[&], Sheyanghe[&], Jinjiang[&], Wangquanhe[&], Nandujiang[&], Kinabatangan[&], Tutoh[&], Milan[&], Pedas[&], Labuk[&], Agno[&], and Papar[&]. Carbon concentrations are reported as river discharge-weighted average concentrations. - Not available.

the downstream end (outer Lingdingyang, Wanshan Islands, Dangan Islands) can cause significant DIC removal. In August 2005, a strong bloom occurred in the Zhujiang River estuary. This resulted in a DIC removal of up to ~40% of the riverine input (the effective concentration was reduced from 1628 to 984 μmol kg^{-1}; Guo X et al., 2009). Since the blooms generally occur in summer, the DIC removal rate in the Zhujiang River estuary does not exceed 10% annually. Similarly, yearly DIC removal is ~10% in the Huanghe River estuary (Zhang and Zhang, 2007). Considering that biogeochemical processes can either produce or reduce DIC in estuaries, we assume that the DIC flux into an estuary is

identical to the flux from the estuary to the marginal sea with an error less than 10%. In addition, the removal rate of POC in the estuaries of China has not been reported. Studies in the Zhujiang River estuary showed that at least 35% of the POC from the Zhujiang River was removed in the Lingdingyang (ignoring the contribution of on-site POC export; He Biyan, unpublished data). Therefore, we assigned the estuarine POC removal rate as 35%, and the DOC removal rate as 10% (Dai et al., 2012). Due to the minor riverine PIC flux, we ignore PIC removal or addition in the estuaries. Overall, the riverine fluxes of DIC, DOC, PIC, and POC into the China Seas were calculated to be 40.8±4.8, 6.19±1.1, 4.05±3.7 and 8.62±1.8 Tg C yr^{-1}, respectively. This adds to a total carbon flux of 59.6±6.4 Tg C yr^{-1}.

2.2.2 *Air-sea CO_2 fluxes in estuaries*

Since the turbidity in estuaries is generally high, weak light availability limits nutrient uptake and phytoplankton growth in most estuaries. pCO_2 in upper estuaries is usually high, primarily due to limited biological uptake and strong aerobic respiration of terrestrial organic carbon. Therefore, most estuaries emit CO_2 to the atmosphere (Chen et al., 2013). To evaluate the CO_2 exchange fluxes in estuaries connecting to the China Seas, we first calculated CO_2 fluxes in the three largest river estuaries (the Changjiang River, the Zhujiang River, and the Huanghe River estuaries) based on published data. Then we estimated the CO_2 flux in all China's estuaries, as a whole, based on the area-weighted CO_2 flux of these river estuaries and the total surface area of all the estuaries.

Surface water pCO_2 in the upper Changjiang estuary ranged from 650–1440 μatm. pCO_2 in the Huangpu River, a highly human perturbed downstream tributary of the Changjiang flowing through Shanghai, was higher, ranging from 1000–4600 μatm (Zhai et al., 2007). In the estuarine mixing zone, pCO_2 ranged from 200–1000 μatm (Zhai et al., 2007). The inner Changjiang estuary (121°–122°E, excluding the Huangpu River and waters around Shanghai) emitted 15.5 mol m^{-2} yr^{-1} CO_2 to the atmosphere (Zhai et al., 2007), which is equivalent to 0.30±0.11 Tg C yr^{-1} (over a surface area of 1600 km^2), or 1.6% of the DIC flux to the ECS from the Changjiang River (18.48 Tg C yr^{-1}; Zhai et al., 2007).

The Zhujiang River estuary consists of three sub-estuaries: the Lingdingyang, Modaomen, and Huangmaohai. The Lingdingyang is surrounded by large metropolitan areas such as Guangzhou and Hong Kong. Surface water pCO_2 in the upper Lingdingyang reached as high as 8000 μatm, much higher than the other two sub-estuaries (<2000 μatm; Guo X et al., 2009). The high pCO_2 in the upper Lingdingyang is mainly attributed to strong aerobic respiration and nitrification (Dai et al., 2006, 2008). pCO_2 spatial distribution is dominated by mixing between high-pCO_2 estuarine water and low-pCO_2 seawater in the mid Lingdingyang, though the magnitude is controlled by net community production (NCP) in the lower Lingdingyang (Guo X et al., 2009). Correspondingly, the upper Lingdingyang is a strong CO_2 source (50–350 mmol m^{-2} d^{-1} or 18–128 mol m^{-2} yr^{-1}), while the lower Lingdingyang is a CO_2 sink during summer (Guo X et al., 2009). The Zhujiang River estuary experiences large seasonal variations in air-sea CO_2 fluxes, and area-weighted CO_2 fluxes are 6 times higher in the summer than in winter. As the surface area of the upper Lingdingyang is small, the entire Zhujiang River estuary is a moderate CO_2 source annually (6.92 mol m^{-2} yr^{-1}). The surface area of the Zhujiang River estuary is 4360 km^2 and it emits 0.36±0.14 Tg C yr^{-1} as CO_2 to the atmosphere, equivalent to 6% of the DIC flux (5.76 Tg C yr^{-1}) from the Zhujiang River estuary to the SCS (Guo X et al., 2008, 2009).

The limited data from the Huanghe River estuary suggests surface water pCO_2 is lower than both the Changjiang and Zhujiang river estuaries. pCO_2 ranged from 380–700 μatm in May and September of 2009 (Liu et al., 2014). If the same air-sea exchange rate as the Changjiang inner estuary is taken (~8 cm h^{-1}; Zhai et al., 2007), the estimated air-sea CO_2 flux in the Huanghe River estuary is 4.2 mol m^{-2} yr^{-1}. Assuming a surface area of 35 km^2, the Yellow River estuary emits 0.002±0.001 Tg C yr^{-1} as CO_2 to the atmosphere.

The area-weighted air-sea CO_2 flux of the above three estuaries is 9.19 mol C m^{-2} yr^{-1}. The total area of the other 38 estuaries discharging into the China Seas, such as the Hanjiang, Qinjiang and Minjiang, is 670 km^2 (determined as the area of the channel from the estuary mouth to 20 km upstream). If 9.19 mol C m^{-2} yr^{-1} is taken as the average CO_2 flux in the estuaries, the 38 estuaries (excluding the three large river estuaries) emit 0.07 Tg C yr^{-1} of CO_2 to the atmosphere. In total, China's estuaries emit 0.74±0.18 Tg C yr^{-1} of CO_2 to the atmosphere (Figure 4).

2.3 POC export flux

POC export flux is considered to be equivalent to NCP under steady state conditions (Cai et al., 2008). It is typically used to evaluate the efficiency of the biological production, which greatly modulates the CO_2 level in the atmosphere. There are several methods to quantify POC export flux, including but not limited to: sediment trap deployment (Chen et al., 1998; Ho et al., 2009), $^{234}Th/^{238}U$, $^{210}Pb/^{226}Ra$, and $^{210}Po/^{210}Pb$ disequilibria (Wei et al., 2011; Chen et al., 2008; Cai et al., 2008, 2015), $^{228}Ra/NO_3$ modeling (Nozaki and Yamamoto, 2001), carbon budgeting (Chou et al., 2006), and ^{15}N tracer-based new production (Dugdale and Wilkerson, 1986). Among them, the last three methods measure the POC fluxes indirectly. Subsequently, they can induce discrepancies when compared with the direct methods on a temporal scale. Thus, we only discussed the results from sediment trap and radiochemistry methodologies, which measure the flux directly and focus on the fluxes in the euphotic zone.

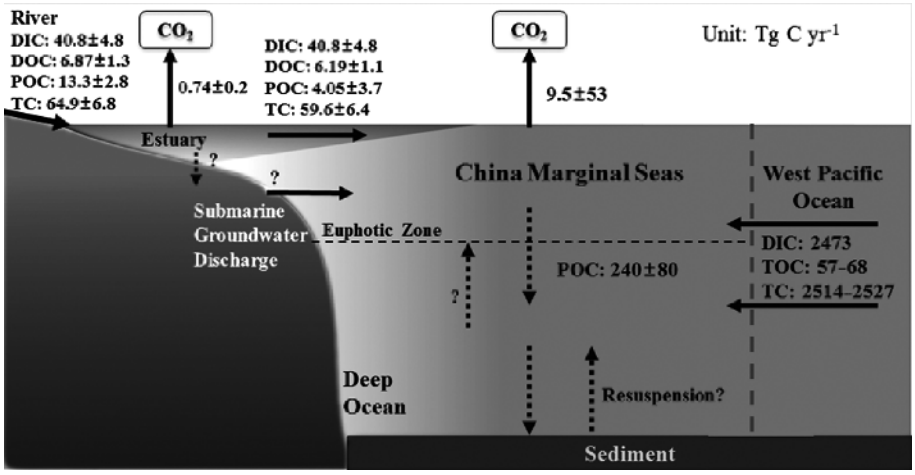

Figure 4 Carbon fluxes in the China Seas (unit: Tg C yr^{-1}). Quantified fluxes across interfaces include air-sea CO_2 fluxes in the China Seas, carbon fluxes (DIC, DOC, POC, TC) from rivers to estuaries and from estuaries to the China Seas, air-sea CO_2 fluxes in Chinese estuaries, POC export fluxes from upper China Seas, and net carbon (DIC, TOC, and TC) fluxes from the West Pacific Ocean to the marginal seas. The carbon fluxes associated with submarine groundwater discharge, sediment burial, and transport into the euphotic layer through diffusion or upwelling are very limited and have not been quantified. The annual average air-sea CO_2 flux in each marginal sea is derived from the product of the air-sea CO_2 flux per unit area from the literature (the references are presented in the caption of Figure 3 and the text) and the total surface area of the marginal sea. The China Seas are a net CO_2 source to the atmosphere, with the degassing CO_2 flux estimated to be 9.5±53 Tg C yr^{-1}. The reported error represents spatial and temporal variations in CO_2 fluxes. Riverine carbon fluxes into the estuaries and China Seas are presented in Table 1 and the text in detail. It should be noted that riverine carbon fluxes into the estuaries exclude the estuaries outside of Chinese borders. In addition, we do not consider Beibu Bay and the Gulf of Thailand when calculating the area of the South China Sea (SCS), and we neglect the carbon exchange fluxes between the SCS and Beibu Bay as well as the Gulf of Thailand. We also do not consider the carbon export from the SCS to the Mindoro Strait and the Karimata Strait.

2.3.1 *South China Sea*

Large variations in POC fluxes in the SCS were observed via different methodologies. On the northern SCS shelf, POC fluxes were mainly derived from $^{234}Th/^{238}U$ disequilibria. Chen (2008) reported the POC flux, as ranging from 5.3–26.6 mmol C m^{-2} d^{-1} with an average of 15±4.6 mmol C m^{-2} d^{-1}. Cai et al. (2015) re-evaluated the POC flux in the same region as Chen (2008) based on high spatial resolution sampling. They reported POC fluxes ranging from 4.6–66.7 mmol C m^{-2} d^{-1}, with an average of 25±1.7 mmol C m^{-2} d^{-1}. In the SCS basin, the POC flux was 9.6–21 mmol C m^{-2} d^{-1} based on $^{234}Th/^{238}U$ disequilibria, 1.8–20 mmol C m^{-2} d^{-1} based on $^{210}Po/^{210}Pb$ disequilibria, and 7.2–21 mmol C m^{-2} d^{-1} based on $^{210}Pb/^{226}Ra$ disequilibria (Wei et al., 2011; Yang et al., 2009). The POC flux derived from sediment traps is 9.8–18.5 mmol C m^{-2} d^{-1} (Ho et al., 2009). Summing the values above, the average POC flux was 14.4±3.6 mmol C m^{-2} d^{-1}. For now, the most comprehensive and highest resolution POC flux values in the northern SCS basin were measured by Cai et al. (2015), and range from 0.8–16.2 mmol C m^{-2} d^{-1}. Therefore, the total observed range of POC fluxes is 0.8–21 mmol C m^{-2} d^{-1}, with an average of 8.7±3.6 mmol C m^{-2} d^{-1}. From the few measurements carried out in the southern SCS basin, the POC flux is approximately 1.7–5.7 mmol C m^{-2} d^{-1} based on both $^{234}Th/^{238}U$ and $^{228}Th/^{228}Ra$ disequilibria (Cai et al., 2002). Cai et al. (2008) pointed out that the spatial variability in POC fluxes is significant, and the average POC flux was 3.8±4.0 mmol C m^{-2} d^{-1} in the southern SCS basin. In general, the POC flux was observed to be higher in the shelf region compared to the basin. Considering seasonal variation, the POC fluxes in the SCS are highest in winter but comparable during other seasons (Wei et al., 2011; Chen, 2008; Cai et al., 2015). Additionally, inter-annual variability may be impacted by ENSO (Li et al., 2017).

The e-ratio (export production to primary production) is typically used to measure the efficiency of the biological pump within a particular area. Although the SCS is oligotrophic, its e-ratio is generally >10%, higher than other subtropical oceans (Wei et al., 2011; Chen et al., 2008). Thus, the efficiency of the biological pump in the SCS is relatively high compared with open ocean. It is proposed that the export fluxes from the euphotic zone of the SCS are mainly controlled by POC stocks, and that export efficiency is positively correlated with diatom abundance, indicating that community structure is important in modulating the downward export of material in the SCS (Cai et al., 2015).

2.3.2 *East China Sea and Yellow Sea*

In the ECS and YS, where the water depths in most regions are shallow (<100 m), diapycnal mixing could reach to the sea bottom under the influence of the northeast monsoon and may last for >3 months. Therefore, intense re-suspension in these two marginal seas creates difficulties in estimating POC fluxes (Dai et al., 2013b). Hung et al. (2013) estimated net POC fluxes of 24.7–65.4, 5.7, and 4.8 mmol C m^{-2} d^{-1} respectively on the inner, mid, and outer shelf, using a simple model to deduct the contribution from re-suspension. In

shallow water (38–88 m) and deep water (118–154 m) regions, the re-suspension ratio could be 57–93% and 27–58%, respectively (Hung et al., 2013; Guo et al., 2010). Based on $^{234}Th/^{238}U$ disequilibria, Zhou (2009) estimated that net POC fluxes in the YS vary within 26.4–52 mmol C m^{-2} d^{-1}, with an average of 37.3±0.9 mmol C m^{-2} d^{-1}. Using floating sediment traps and similar methodology, Zhang et al. (2005) determined POC fluxes of 16 mmol C m^{-2} d^{-1} during the fall and 24.2±3.3 mmol C m^{-2} d^{-1} during the summer (Zhang et al., 2004). Consequently, the average POC flux in the YS was 20.1±4.2 mmol C m^{-2} d^{-1}, and the re-suspension flux reached 16.9 mmol C m^{-2} d^{-1}.

Synthesizing all data presented above, the POC export flux increases with decreasing water depth. POC export fluxes are 20±9.8 mmol C m^{-2} d^{-1} on the SCS shelf, 5.4±2.5 mmol C m^{-2} d^{-1} in the SCS basin, 24.6±22.5 mmol C m^{-2} d^{-1} in the ECS, and 29.2±11.5 mmol C m^{-2} d^{-1} in the YS. This regional trend, SCS<ES<YS, may be caused by the decreased remineralization rate in the YS due to its shallow depth and the large cell diatom dominated community structure. By considering the surface area of the three seas, we determined that annual POC fluxes are 110±40 Tg C yr^{-1} in the SCS, 80±70 Tg C yr^{-1} in the ECS and 50±20 Tg C yr^{-1} in the YS. In summary, the total POC flux in the three China Seas is 240±80 Tg C yr^{-1}.

2.4 Exchange with the Pacific Ocean

Marginal seas are subject to complex material and energy exchanges with the open ocean. For instance, material exchanges between the north Atlantic Ocean and the Caribbean Sea, Gulf of Mexico, and North Sea, significantly affect the carbon fluxes in these marginal seas (Thomas et al., 2005). Meanwhile, marginal seas are characterized by higher rates of biological activities such as primary productivity, providing material sources to the open ocean. For instance, Liu et al. (2000) stated that marginal seas transport a considerable amount of organic carbon to the open ocean; up to 2 Pg C yr^{-1}. Given the high temporal and spatial variability of the exchange between marginal seas and the open ocean, it is difficult to accurately define the material exchange both from observation and simulation, thus becoming a challenging scientific question (Doney, 2010).

With the Kuroshio acting as a link, the Northwest Pacific Ocean-East Asian marginal sea is the most unique open ocean-ocean margin system. Water, energy, and material exchanges between these systems, significantly influence the Northwest Pacific Ocean (NWP) and its adjacent marginal seas (Chen and Wang, 1999; Chen et al., 2006; Chou et al., 2007; Cao and Dai, 2011; Dai et al., 2009; Sheu et al., 2009; Wu et al., 2015; Lu et al., 2015). Chen and Wang (1999) estimated the contribution of the Kuroshio to the nutrient budget in the ECS, and they concluded that the phosphate in the ECS primarily originated from the intrusion of Kuroshio intermediate water.

The annual flux of DOC transported from the ECS to the NWP is between 2–12 Tg C yr^{-1} (Chen and Wang, 1999; Liu et al., 2006, 2010b). The POC outflow flux from the ECS to the adjacent NWP is 0.25 Tg C yr^{-1}. Based on a carbon budget model for the ECS, the DOC, and DIC fluxes from the ECS to the adjacent NWP are estimated to be 50–63 Tg C yr^{-1} (Deng et al., 2006).

The Luzon Strait is a major deep-water channel, allowing exchange between the SCS and the NWP. This exchange is characterized as a "sandwich-like" structure with an inflow from the NWP in the upper and deep layers, and an outflow to the NWP in the intermediate layer (Chao et al., 1996; Gan et al., 2006; Li and Qu, 2006; Qu et al., 2006; Tian et al., 2006). The continuously-replenished deep water in the SCS, originating from the NWP, achieves water balance through the rapid ventilation and persistent net intermediate water outflow (Chao et al., 1996; Li and Qu, 2006). This process can be observed by examining the distribution of TOC (total organic carbon), as an example. The TOC concentration in the upper 200 m of the SCS is lower than that in the NWP. SCS intermediate water (1000–1500 m) has relatively higher TOC values, and SCS TOC concentrations at depths >2000 m are comparable with the NWP deep water (Dai et al., 2009; Wu et al., 2015). Combining the water exchange fluxes and TOC concentrations, we determined that the TOC transport fluxes in the upper, intermediate, and deep layers of the SCS to be −107.1±54.6, 54.7±15.0, and −16.4±13.1 Tg C yr^{-1}, respectively (positive values refer to transport from the SCS to the NWP). The net TOC output is −68.8±58.0 Tg C yr^{-1}. Using this calculation methodology, we also find the exchange fluxes of other materials through the Luzon Strait. The net influxes of DIC, total alkalinity (TA), and Ca^{2+} to the SCS are 2.5 Pg C yr^{-1}, 2.8 Pg C yr^{-1}, and 40 Pg Ca yr^{-1}. The net fluxes of dissolved inorganic nitrogen (DIN), dissolved inorganic phosphorus (DIP), and dissolved silicates (DSi) to the NWP are 7 Tg N yr^{-1}, 4.65 Tg P yr^{-1}, and 137.2 Tg Si yr^{-1}, respectively. The DIC flux transported to the SCS through the deep layer is as high as 984 Tg C yr^{-1}. Together, the total amount of carbon transported from the NWP to the SCS and ECS is 2.5 Pg C yr^{-1}. Given the different C:N:P:Si ratios between the SCS and the NWP, their exchange could result in a significant influence on the biogeochemical cycles of carbon and associated biogenic elements in both the SCS and NPW.

It should be noted that the above flux estimates may have large uncertainties due to limited datasets. In addition, we did not consider carbon export from the SCS via the Mindoro and Karimata straits, and carbon exchanges between the SCS and the Beibu Gulf and Gulf of Thailand.

3. A comparison between the China Seas and other world marginal seas

According to physical-biogeochemical characteristics, the marginal seas can be classified into several provinces (Cai et al., 2006; Dai et al., 2013a). The mid-latitude (30°–60°) non-upwelling marginal seas possess characteristics of a broad shelf; seasonal stratification without strong coastal upwelling. These marginal seas can be further classified into two types: the eutrophic shelves that receive substantial anthropogenic nutrients, and the mesotrophic shelves that receive relatively less terrestrially-derived nutrients (Cai et al., 2006; Dai et al., 2013a). The former include the Mid Atlantic Bight (absorbing 2.65 Tg C yr^{-1} of CO_2; Cai et al., 2006; DeGrandpre et al., 2002), the Baltic Sea (absorbing 4.21 Tg C yr^{-1}; Thomas and Schneider, 1999), the Sea of Japan (absorbing 29.6 Tg C yr^{-1} of CO_2; Choi et al., 2012; Kang et al., 2010), the North Sea (absorbing 8.46 Tg C yr^{-1} of CO_2; Thomas et al., 2004), and the Mediterranean Sea shelf (absorbing 3.51 Tg C yr^{-1} of CO_2; Bégovic and Copin-Montégut, 2002; Borges et al., 2006; Copin-Montégut et al., 2004). Overall, eutrophic shelves in the mid-latitude non-upwelling marginal seas absorbed 81.7 Tg C yr^{-1} of CO_2 from atmosphere (Dai et al., 2013). Examples of mesotrophic shelves are the Bering Sea shelf (absorbing 23.8 Tg C yr^{-1} of CO_2; Bates et al., 2011), the Patagonian Sea in South America (absorbing 16.2 Tg C yr^{-1} of CO_2; Bianchi et al., 2009), and the Gulf of Maine (releasing 0.46 Tg C yr^{-1} of CO_2 to atmosphere; Vandemark et al., 2011). This type of shelf absorbed 168.2 Tg C yr^{-1} of CO_2 from atmosphere (Dai et al., 2013a).

Although the low-latitude (0°–30°) western boundary shelves are also characterized by non-upwelling, the CO_2 fluxes are different from mid-latitude marginal seas. These low latitude western marginal seas feature high temperatures and large riverine inputs of both inorganic and organic carbon. As a whole, this type of marginal sea was a CO_2 source of 29.8 Tg C yr^{-1} (Dai et al., 2013a). Examples of low-latitude marginal seas include the Brazil shelf (releasing 11.5 Tg C yr^{-1} of CO_2; Ito et al., 2005) and the west Florida shelf (releasing 4.28 Tg C yr^{-1} of CO_2; Cai et al., 2006).

The eastern boundary marginal seas are also classified into two types: the low-latitude and mid-latitude marginal seas. The eastern boundary marginal seas are usually characterized by narrow shelves and coastal upwelling. The low-latitude upwelling systems are typically CO_2 sources due mainly to both high temperatures and upwelling. This type of marginal sea acted as a CO_2 source of 53.1 Tg C yr^{-1} (Dai et al., 2013a). Examples of low-latitude upwelling systems include the Peruvian upwelling system (releasing 54.7 Tg C yr^{-1} of CO_2 to atmosphere; Friederich et al., 2008) and the Chilean upwelling system (releasing 1.94 Tg C yr^{-1} of CO_2; Torres et al., 2003, 2011). The CO_2 sources of the mid-latitude upwelling systems are much weaker than those of the low-latitude upwelling systems and show larger seasonal variability. These marginal seas released 11.8 Tg C yr^{-1} of CO_2 to atmosphere (Dai et al., 2013a). Examples of mid-latitude upwelling systems include upwelling off the coast of California (releasing 2.70 Tg C yr^{-1} of CO_2; Friederich et al., 2002; Hales et al., 2005), and the southern Bering Sea slope (releasing 16.4 Tg C yr^{-1} of CO_2; Fransson et al., 2006). Although the mid-latitude upwelling systems are usually CO_2 sources, the Oregon shelf (absorbing 4.36 Tg C yr^{-1}; Evans et al., 2011) and the western Canadian coast (absorbing 1.55 Tg C yr^{-1} of CO_2; Evans et al., 2012) are CO_2 sinks.

High-latitude (60°–90°) marginal seas are also called phototrophic marginal seas, as primary production in these regions is usually limited by the weak light availability. Although receiving a large amount of riverine inputs of organic carbon, the phototrophic-Arctic marginal seas are a CO_2 sink due to the low temperatures (−202.5 Tg C yr^{-1}; Dai et al., 2013a). The Greenland-Norwegian Seas (absorbing 118.8 Tg C yr^{-1} of CO_2 from atmosphere; Anderson et al., 2000; Hood et al., 1999; Nakaoka et al., 2006; Skjelvan et al., 1999; Slagstad et al., 1999), the Barents Sea (absorbing 68.0 Tg C yr^{-1} of CO_2; Nakaoka et al., 2006; Omar et al., 2007), and the Chukchi Sea (absorbing 9.65 Tg C yr^{-1} of CO_2; Arrigo et al., 2010; Bates, 2006; Gao et al., 2012; Semiletov et al., 2007) are examples of this type of marginal sea. The Antarctic marginal seas were also a CO_2 sink of 5.3 Tg C yr^{-1} because of low temperatures, although they are also influenced by upwelling (Dai et al., 2013a and references therein).

As for the China Seas, the YS and the ECS are mid-latitude eutrophic shelves, and the SCS belongs to low-latitude western boundary shelves.

4. Future research

4.1 Long-term observations

Although a large number of regional observations of carbon fluxes have been conducted over the last 20 years, large uncertainties remain in evaluating the air-sea CO_2 fluxes in the China Seas. In the BS and the NYS, the CO_2 source-sink patterns are still quite uncertain. Even though the basic source-sink patterns of CO_2 have been determined in the SCS and ECS, the temporal and spatial resolution remain insufficient mainly due to a lack of long-term time-series observations.

Current estimates of air-sea CO_2 fluxes are generally based on measurements of pCO_2 disparity (the difference between surface water pCO_2 and atmospheric pCO_2). Given that atmospheric pCO_2 is relatively homogeneous and constant, the

accurate measurement of surface water pCO_2 thus becomes the determining factor for estimating the air-sea CO_2 flux (Wang et al., 2014). Calculated average surface water pCO_2 estimates are usually based on gridded pCO_2 data. The uncertainties in the gridded pCO_2 data mainly originate from three sources (Wang et al., 2014): (1) analytical error in the pCO_2 measurement, (2) spatial variance, and (3) the bias resulting from under-sampling. Analytical error in surface water pCO_2 can be controlled within 1%, making the uncertainty of the CO_2 flux mainly related to (2) and (3). Wang et al. (2014) developed a method to quantitatively estimate the three uncertainties in surface water pCO_2 gridded data using both observational and remote sensing data. They found that spatial variances of surface water pCO_2 were the dominant source of uncertainty on the ECS shelf during summer. Thus, identifying and quantifying the sources of uncertainty for pCO_2 gridded data are essential for accurately estimating the air-sea CO_2 fluxes and the ocean's carbon budget. It should be noted that the inherent spatial variance cannot be reduced by increasing the observation frequency, but it is useful to identify different sources of uncertainty in planning the spatial and temporal resolution of observations.

It is a huge challenge to precisely predict the changes in the Earth's climate system and carbon cycle at both regional and global dimensions across different time-scales (e.g., from annual to decadal scales). However, little is known about the carbon cycle in the China Seas over these timescales. Taking the Changjiang River estuary as an example, Chou et al. (2013) reported that the surface water pCO_2 during summer showed a decreasing trend from the 1990s to 2000s. They attributed this trend to the increasing biological DIC uptake as a result of enhanced photosynthesis via eutrophication. Moreover, the CO_2 sink during winter for the inner shelf of ECS near the Changjiang estuary has decreased due to global warming (Chou et al., 2013). However, this statement needs to be further validated by long-term observations.

Remote sensing is a critically important tool in improving the spatial and temporal coverage of surface water pCO_2 observations. As such, many efforts have been made to estimate sea surface pCO_2 and air-sea CO_2 fluxes from space by developing empirical relationships between pCO_2 and satellite-derived parameters (Jo et al., 2012 and references therein). Bai et al. (2015) proposed a "mechanistic semi-analytic algorithm" (MeSAA) to estimate sea surface pCO_2 in river-dominated coastal oceans using satellite data. Observed pCO_2 can be analytically expressed as the sum of individual components contributed by major factors such as thermodynamics, water mass mixing, and biological processes. It must be pointed out that applications of these approaches to marginal seas worldwide remain challenging due to the high spatio-temporal variations and their intrinsic controls in both physics and biogeochemistry in different marginal seas.

4.2 Towards a conceptual framework of marginal sea carbon cycling

Currently, there are still difficulties in reliably simulating biogeochemical processes and carbon cycling in marginal seas using numerical models. Dai et al. (2013a) developed an alternative approach by coupling physical and biogeochemical processes, and carbon and nutrients in attempting to build up a semi-quantitative diagnostic method and a conceptual framework of marginal sea carbon cycling. The complexity in simulating marginal sea carbon cycling is owed to its modulation by both terrestrial inputs and their exchanges with the open ocean. Therefore, the carbon cycle in marginal seas is a function of both exogenous inputs (terrestrial inputs and exchange with the open ocean) and internal processes (thermodynamic and the biological pump). The net CO_2 sink/source term in a marginal sea is dependent on the balance between the relative external contribution of DIC and nutrients to the upper layer, as well as biogeochemical consumption therein. OceMar was validated in the SCS, the Caribbean Sea, and the upwelling system off the coast of California (Dai et al., 2013a; Cao et al., 2014). Recently, Chou et al. (2017) also verified OceMar in the Peter the Great Bay, located in the northern Sea of Japan. It should be pointed out that this method is based on the assumption of steady state conditions; i.e. the time-scale of the mixing of water masses is the same or similar with that of the biogeochemical processes (see details in Dai et al., 2013a and Cao et al., 2014).

4.3 Carbon fluxes and mechanisms across the land-sea aquatic continuum

As previously stated, marginal seas are located in transitional zones between land and open ocean. These regions involve complex, dynamic, and multi-scale processes. Here we address two aspects that are not well-constrained on the role of the land-sea transition zone in the China Seas carbon cycle.

4.3.1 Submarine groundwater discharge (SGD)

Over the last two decades, in addition to rivers, SGD has been identified as a critical component of the land-sea interactions. Also, subterranean estuaries (STE) constitutes another "reactor" in this transition zone (Moore, 1999). Groundwater is often enriched in organic carbon. For example, in a STE in the Gulf of Mexico, the terrestrial groundwater associated DOC flux was equivalent to 25% of the total DOC inputs to the adjacent coastal ocean (Santos et al., 2009). Based on a limited dataset, SGD provided 11–22 Tg C yr^{-1} of DOC to the coastal ocean globally (Dai et al., 2012). However, SGD-derived DOC fluxes to the China estuaries and adjacent marginal seas have not yet been reported. Moreover, pCO_2 is generally elevated in the regional

groundwater by approximately three orders of magnitude above atmospheric pCO_2 (Gagan et al., 2002; Cai et al., 2003), suggesting SGD is an important DIC source to the coastal ocean (Liu Q et al., 2014; Sadat-Noori et al., 2016). For instance, the SGD-DIC flux to the northern SCS shelf during summer accounts for 23–53% of the DIC flux supplied by the Zhujiang River (Liu et al., 2012), and SGD may have a significant impact on the carbonate system in the shelf waters. The DIC flux delivered by SGD to the Jiulong River estuary is equivalent to 45–110% of the contribution from the Jiulong River (Wang et al., 2015). Consequently, SGD as a source of terrestrial carbon, is often overlooked and should be considered in the carbon budget at a regional or global scale in the future.

4.3.2 Coastal wetlands

Wetland ecosystems are characterized by high rates of primary productivity with slow organic matter decomposition. The carbon burial flux in this system has been estimated to be as high as 100 Tg C yr^{-1} globally (Hopkinson et al., 2012). As a large "blue carbon" sink, their impact on the global carbon cycle has become an important topic in recent years (Sutula et al., 2003; Søvik and Kløve, 2007; Zhang et al., 2008; Sanders et al., 2016). China has the largest wetland area in Asia with a total area of 3.85×10^7 km^2 (Duan et al., 2008) and a coastal wetland area of ~5.94×10^4 km^2 (Cao et al., 2013). Current studies have shown that the burial rate of organic carbon in various types of swamp wetlands (peatland, freshwater marsh, inland salt marsh, coastal salt marsh, and forest wetland) in China is 4.91 Tg C yr^{-1} (Duan et al., 2008). The highest carbon sequestration rate (CSR) in the wetlands can be found in mangroves and coastal salt marshes (Alongi, 2014). Coastal wetlands are extremely complex ecosystems with respect to carbon fluxes. Wetland vegetation can absorb atmospheric CO_2 via photosynthesis, and vegetation litter forms peat and humus as it becomes part of the soil. While some of the carbon is buried in the soil, a large portion is also re-released as CO_2 and CH_4 into the atmosphere through respiration. The remaining carbon discharges into the ocean by lateral transport through surface and subterranean estuaries, which significantly affects the marine carbon cycle.

In recognition of the critical importance of wetland ecosystems in global carbon sequestration, many studies focus on the evaluation of CSR, which is estimated based on sedimentation rates and total organic carbon content of the soil (Alongi, 2014; Alongi et al., 2005; Liu H et al., 2014). This evaluation is based on the assumption that these soils solely fix atmospheric CO_2. However, coastal wetland systems could also be affected by lateral transport at the surface and through groundwater/porewater exchange. In other words, currently estimated CSRs and carbon sequestration capacities may include carbon both fixed from the atmosphere and from lateral transport. Bouillon et al. (2008) and Alongi (2009) observed an imbalance between carbon sources and sinks in mangrove systems globally, and a missing carbon sink that reaches up to 110 Tg C yr^{-1}. While the mechanisms behind these imbalances are still unclear, it remains a possibility that all the imports and exports of carbon within these systems are not fully considered, particularly the lateral transport of DIC resulting from surface and porewater exchange (Maher et al., 2013; Alongi, 2014). Recently, based on scaling measurements from a few mangrove systems in Australia, Sippo et al. (2017) estimated that the lateral DIC flux in mangrove systems globally was 43±12 Tg C yr^{-1}. This estimate accounts for one-third of the missing carbon sinks. Therefore, lateral transport could be an important carbon sink in coastal wetland systems and may also impact the coastal ocean carbon cycle. Yet, its accurate quantification is still very challenging and accurate estimates are scarce. In China, systematic studies of carbon storage and cycling have been only carried out on tidal flat wetlands in the Changjiang estuary (Alongi et al., 1999, 2005; Cheng et al., 2010; Guo H Q et al., 2009). Thus, it is premature to comprehensively evaluate the contribution of coastal wetlands to the regional carbon cycle in China. As such, it remains urgent to strengthen research on the carbon budget of coastal wetland systems in the future.

4.4 Perturbation of the carbon cycle in marginal seas

The effect of human activities on the ocean's carbon cycle has been a hot topic in recent years. However, the driving forces are complex and variable (Le Quéré et al., 2017; Regnier et al., 2013). Since marginal seas are located where the land, ocean, and atmosphere interact, human activities can affect all three spheres. For example, in the terrestrial environment, human activities (including the change of land use patterns, embankment construction, wastewater discharge, and marsh dredging) are changing or have changed carbon sources, cycling and budgets in estuaries. Subsequently, this has resulted in variations of riverine carbon fluxes to the ocean (Regnier et al., 2013). In addition, agricultural activities and land use change largely enhance the nutrient inputs to rivers. This in turn, increases primary productivity and the accumulation of organic carbon in estuaries and the continental shelf. This creates a situation, where consumption of oxygen as organic carbon is degraded, with the transpiration of subsequent exacerbations of hypoxic events and ocean acidification (Cai et al., 2011; Doney, 2010; Wang et al., 2016).

Acknowledgements *We are grateful to Dr. Zhiqiang Liu (Hong Kong University of Science and Technology) for calculating the area of 38 estuaries and Yan Yang for references compiling. This research was supported by the National Natural Science Foundation of China (Grant Nos.*

91328202 & 91428308), the Major Scientific Research Program of the Ministry of Science and Technology (Grant No. 2015CB954001), the Marine Public Welfare Project of the State Oceanic Administration (Grant No. 201505003-3), and the Global Change Program (Grant No. GASI-03-01-02-02).

References

Alongi D M. 2009. The Energetics of Mangrove Forests. New York: Springer. 216

Alongi D M. 2014. Carbon cycling and storage in mangrove forests. Annu Rev Mar Sci, 6: 195–219

Alongi D M, Tirendi F, Dixon P, Trott L A, Brunskill G J. 1999. Mineralization of organic matter in intertidal sediments of a tropical semi-enclosed delta. Estuar Coast Shelf Sci, 48: 451–467

Alongi D M, Pfitzner J, Trott L A, Tirendi F, Dixon P, Klumpp D W. 2005. Rapid sediment accumulation and microbial mineralization in forests of the mangrove Kandelia candel in the Jiulongjiang Estuary, China. Estuar Coast Shelf Sci, 63: 605–618

Anderson L G, Drange H, Chierici M, Fransson A, Johannessen T, Skjelvan I, Rey F. 2000. Annual carbon fluxes in the upper Greenland Sea based on measurements and a box-model approach. Tellus Ser B-Chem Phys Meteorol, 52: 1013–1024

Arrigo K R, Pabi S, van Dijken G L, Maslowski W. 2010. Air-sea flux of CO_2 in the Arctic Ocean, 1998–2003. J Geophys Res, 115: G04024

Bai Y, Cai W J, He X, Zhai W, Pan D, Dai M, Yu P. 2015. A mechanistic semi-analytical method for remotely sensing sea surface pCO_2 in river-dominated coastal oceans: A case study from the East China Sea. J Geophys Res, 120: 2331–2349

Bates N R. 2006. Air-sea CO_2 fluxes and the continental shelf pump of carbon in the Chukchi Sea adjacent to the Arctic Ocean. J Geophys Res, 111: C10013

Bates N, Cai W J, Mathis J. 2011. The ocean carbon cycle in the western Arctic Ocean: Distributions and air-sea fluxes of carbon dioxide. Oceanography, 24: 186–201

Bégovic M, Copin-Montégut C. 2002. Processes controlling annual variations in the partial pressure of CO_2 in surface waters of the central northwestern Mediterranean Sea (Dyfamed site). Deep-Sea Res Part II-Top Stud Oceanogr, 49: 2031–2047

Bianchi A A, Pino D R, Perlender H G I, Osiroff A P, Segura V, Lutz V, Clara M L, Balestrini C F, Piola A R. 2009. Annual balance and seasonal variability of sea-air CO_2 fluxes in the Patagonia Sea: Their relationship with fronts and chlorophyll distribution. J Geophys Res, 114: C03018

Borges A V. 2011. Present day carbon dioxide fluxes in the coastal ocean and possible feedbacks under global change. In: Duarte P, Santana-Casiano J M, eds. Oceans and the Atmospheric Carbon Content. Dordrecht: Springer. 47–77

Borges A V, Delille B, Frankignoulle M. 2005. Budgeting sinks and sources of CO_2 in the coastal ocean: Diversity of ecosystems counts. Geophys Res Lett, 32: L14601

Borges A V, Schiettecatte L S, Abril G, Delille B, Gazeau F. 2006. Carbon dioxide in European coastal waters. Estuar Coast Shelf Sci, 70: 375–387

Bouillon S, Borges A V, Castañeda-Moya E, Diele K, Dittmar T, Duke N C, Kristensen E, Lee S Y, Marchand C, Middelburg J J, Rivera-Monroy V H, Smith Iii T J, Twilley R R. 2008. Mangrove production and carbon sinks: A revision of global budget estimates. Glob Biogeochem Cycle, 22: GB2013

Canadell J G, Ciais P, Dhakal S, Dolman H, Friedlingstein P, Gurney K R, Held A, Jackson R B, Le Quéré C, Malone E L, Ojima D S, Patwardhan A, Peters G P, Raupach M R. 2010. Interactions of the carbon cycle, human activity, and the climate system: A research portfolio. Curr Opin Environ Sustainability, 2: 301–311

Cai P, Chen W, Dai M, Wan Z, Wang D, Li Q, Tang T, Lv D. 2008. A high-resolution study of particle export in the southern South China Sea based on ^{234}Th:^{238}U disequilibrium. J Geophys Res, 113: C04019

Cai P, Huang Y, Chen M, Guo L, Liu G, Qiu Y. 2002. New production based on ^{228}Ra-derived nutrient budgets and thorium-estimated POC export at the intercalibration station in the South China Sea. Deep-Sea Res Part I-Oceanogr Res Pap, 49: 53–66

Cai P, Zhao D, Wang L, Huang B, Dai M. 2015. Role of particle stock and phytoplankton community structure in regulating particulate organic carbon export in a large marginal sea. J Geophys Res, 120: 2063–2095

Cai W J. 2011. Estuarine and coastal ocean carbon paradox: CO_2 sinks or sites of terrestrial carbon incineration? Annu Rev Mar Sci, 3: 123–145

Cai W J, Dai M. 2004. Comment on "enhanced open ocean storage of CO_2 from shelf sea pumping". Science, 306: 1477c

Cai W J, Dai M, Wang Y. 2006. Air-sea exchange of carbon dioxide in ocean margins: A province-based synthesis. Geophys Res Lett, 33: L12603

Cai W J, Hu X, Huang W J, Murrell M C, Lehrter J C, Lohrenz S E, Chou W C, Zhai W, Hollibaugh J T, Wang Y, Zhao P, Guo X, Gundersen K, Dai M, Gong G C. 2011. Acidification of subsurface coastal waters enhanced by eutrophication. Nat Geosci, 4: 766–770

Cai W J, Wang Y, Krest J, Moore W S. 2003. The geochemistry of dissolved inorganic carbon in a surficial groundwater aquifer in North Inlet, South Carolina, and the carbon fluxes to the coastal ocean. Geochim Cosmochim Acta, 67: 631–639

Cao L, Song J, Li X, Yuan H, Li N, Duan L. 2013. Research progresses in carbon budget and carbon cycle of the coastal salt marshes in China (in Chinese). Acta Ecol Sin, 33: 5141–5152

Cao Z, Dai M. 2011. Shallow-depth $CaCO_3$ dissolution: Evidence from excess calcium in the South China Sea and its export to the Pacific Ocean. Glob Biogeochem Cycle, 25: GB2019

Cao Z, Dai M, Evans W, Gan J, Feely R. 2014. Diagnosing CO_2 fluxes in the upwelling system off the Oregon-California coast. Biogeosciences, 11: 6341–6354

Chao S Y, Shaw P T, Wu S Y. 1996. Deep water ventilation in the South China Sea. Deep-Sea Res Part I-Oceanogr Res Pap, 43: 445–466

Chen C T A, Borges A V. 2009. Reconciling opposing views on carbon cycling in the coastal ocean: Continental shelves as sinks and near-shore ecosystems as sources of atmospheric CO_2. Deep-Sea Res Part II-Top Stud Oceanogr, 56: 578–590

Chen C T A, Huang T H, Chen Y C, Bai Y, He X, Kang Y. 2013. Air-sea exchanges of CO_2 in the world's coastal seas. Biogeosciences, 10: 6509–6544

Chen C T A, Wang S L. 1999. Carbon, alkalinity and nutrient budgets on the East China Sea continental shelf. J Geophys Res, 104: 20675–20686

Chen C T A, Wang S L, Chou W C, Sheu D D. 2006. Carbonate chemistry and projected future changes in pH and $CaCO_3$ saturation state of the South China Sea. Mar Chem, 101: 277–305

Chen J, Zheng L, Wiesner M G, Chen R, Zheng Y, Wong H K. 1998. Estimations of primary production and export production in the South China Sea based on sediment trap experiments. Chin Sci Bull, 43: 583–586

Chen W. 2008. On the export fluxes, seasonality and controls of particulate organic carbon in the Northern South China Sea (in Chinese). Doctoral Dissertation. Xiamen: Xiamen University

Chen W, Cai P, Dai M, Wei J. 2008. ^{234}Th/^{238}U disequilibrium and particulate organic carbon export in the northern South China Sea. J Oceanogr, 64: 417–428

Cheng X L, Luo Y Q, Xu Q, Lin G H, Zhang Q F, Chen J K, Li B. 2010. Seasonal variation in CH_4 emission and its ^{13}C-isotopic signature from *Spartina alterniflora* and *Scirpus mariqueter* soils in an estuarine wetland. Plant Soil, 327: 85–94

Choi S H, Kim D, Shim J H, Kim K H, Min H S, Kim K R. 2012. Seasonal variations of surface fCO_2 and sea-air CO_2 fluxes in the Ulleung Basin of the East/Japan Sea. Terr Atmos Ocean Sci, 23: 343–353

Chou W C, Chen Y L L, Sheu D D, Shih Y Y, Han C A, Cho C L, Tseng C M, Yang Y J. 2006. Estimated net community production during the summertime at the SEATS time-series study site, northern South China Sea: Implications for nitrogen fixation. Geophys Res Lett, 33: L22610

Chou W C, Gong G C, Hung C C, Wu Y H. 2013. Carbonate mineral

saturation states in the East China Sea: Present conditions and future scenarios. Biogeosciences, 10: 6453–6467
Chou W C, Gong G C, Sheu D D, Hung C C, Tseng T F. 2009. Surface distributions of carbon chemistry parameters in the East China Sea in summer 2007. J Geophys Res, 114: C07026
Chou W C, Gong G C, Tseng C M, Sheu D D, Hung C C, Chang L P, Wang L W. 2011. The carbonate system in the East China Sea in winter. Mar Chem, 123: 44–55
Chou W C, Sheu D D D, Chen C T A, Wang S L, Tseng C M. 2005. Seasonal variability of carbon chemistry at the SEATS site, northern South China Sea between 2002 and 2003. Terr Atmos Ocean Sci, 16: 445–465
Chou W C, Sheu D D, Chen C T A, Wen L S, Yang Y, Wei C L. 2007. Transport of the South China Sea subsurface water outflow and its influence on carbon chemistry of Kuroshio waters off southeastern Taiwan. J Geophys Res, 112: C12008
Chou W C, Tishchenko P Y, Chuang K Y, Gong G C, Shkirnikova E M, Tishchenko P P. 2017. The contrasting behaviors of CO_2 systems in river-dominated and ocean-dominated continental shelves: A case study in the East China Sea and the Peter the Great Bay of the Japan/East Sea in summer 2014. Mar Chem, 195: 50–60
Ciais P, Sabine C, Bala G, Bopp L, Brovkin V, Canadell J, Chhabra A, DeFries R, Galloway J, Heimann M, Jones C, Le Quéré C, Myneni R B, Piao S, Thornton P. 2013. Carbon and other biogeochemical cycles. In: Stocker T F, Qin D, Planttner G-K, Tignor M, Allen S K, Boschung J, Nauels A, Xia Y, Bex V, Midgley P M, eds. Climate Change 2013: The Physical Science Basis. Contribution of Working Group I to the Fifth Assessment Report of the Intergovernmental Panel on Climate Change. Cambridge: Cambridge University Press. 465–570
Copin-Montégut C, Bégovic M, Merlivat L. 2004. Variability of the partial pressure of CO_2 on diel to annual time scales in the Northwestern Mediterranean Sea. Mar Chem, 85: 169–189
Dai A. 2016. Historical and future changes in streamflow and continental runoff: A review. In: Tang Q, Oki T, eds. Terrestrial Water Cycle and Climate Change: Natural and Human-Induced Impacts, Geophysical Monograph 221. AGU: John Wiley & Sons. 17–37
Dai M, Yin Z. 2016. Marine carbon cycle. In: Chinese Academy of Sciences, ed. China Discipline Development Strategy: Marine Science (in Chinese). Beijing: Science Press. 199–221
Dai M, Cao Z, Guo X, Zhai W, Liu Z, Yin Z, Xu Y, Gan J, Hu J, Du C. 2013a. Why are some marginal seas sources of atmospheric CO_2? Geophys Res Lett, 40: 2154–2158
Dai M, Guo X, Zhai W, Yuan L, Wang B, Wang L, Cai P, Tang T, Cai W J. 2006. Oxygen depletion in the upper reach of the Pearl River estuary during a winter drought. Mar Chem, 102: 159–169
Dai M, Meng F, Tang T, Kao S J, Lin J, Chen J, Huang-Chuan J, Tian J, Gan J, Yang S. 2009. Excess total organic carbon in the intermediate water of the South China Sea and its export to the North Pacific. Geochem Geophys Geosyst, 10: Q12002
Dai M, Wang L, Guo X, Zhai W, Li Q, He B, Kao S J. 2008. Nitrification and inorganic nitrogen distribution in a large perturbed river/estuarine system: The Pearl River Estuary, China. Biogeosciences, 5: 1227–1244
Dai M, Yin Z, Meng F, Liu Q, Cai W J. 2012. Spatial distribution of riverine DOC inputs to the ocean: an updated global synthesis. Curr Opin Env Sust, 4: 170–178
Dai M, Zhai W, Lu Z, Cai P, Cai W J, Hong H. 2004. Regional studies of carbon cycles in China: Progress and perspectives (in Chinese). Adv Earth Sci, 19: 120–130
Dai M, Zhai W, Xu Y, Li Q, Han A, Zheng N, Zheng N, Zhou K, Meng F, Lin H, Guo X, Wang X. 2013b. Marine Chemistry. In: Wang Y, Liu R, Su J, eds. China Marine Geography (in Chinese). Beijing: Science Press. 194–244
DeGrandpre M D, Olbu G J, Beatty C M, Hammar T R. 2002. Air-sea CO_2 fluxes on the US Middle Atlantic Bight. Deep-Sea Res Part II-Top Stud Oceanogr, 49: 4355–4367
Deng B, Zhang J, Wu Y. 2006. Recent sediment accumulation and carbon burial in the East China Sea. Glob Biogeochem Cycle, 20: GB3014
DeVries T, Holzer M, Primeau F. 2017. Recent increase in oceanic carbon uptake driven by weaker upper-ocean overturning. Nature, 542: 215–218
Doney S C. 2010. The growing human footprint on coastal and open-ocean biogeochemistry. Science, 328: 1512–1516
Duan X, Wang X, Fei L, Ouyang Z. 2008. Primary evaluation of carbon sequestration potential of wetlands in China. Acta Ecol Sin, 28: 463–469
Dugdale R C, Wilkerson F P. 1986. The use of ^{15}N to measure nitrogen uptake in eutrophic oceans; experimental considerations. Limnol Oceanogr, 31: 673–689
Elderfield H. 2002. Climate change: Carbonate mysteries. Science, 296: 1618–1621
Evans W, Hales B, Strutton P G. 2011. Seasonal cycle of surface ocean pCO_2 on the Oregon shelf. J Geophys Res, 116: C05012
Evans W, Hales B, Strutton P G, Ianson D. 2012. Sea-air CO_2 fluxes in the western Canadian coastal ocean. Prog Oceanogr, 101: 78–91
Falkowski P, Scholes R J, Boyle E, Canadell J, Canfield D, Elser J, Gruber N, Hibbard K, Högberg P, Linder S, Mackenzie F T, Moore I I I B, Pedersen T, Rosenthal Y, Seitzinger S, Smetacek V, Steffen W. 2000. The global carbon cycle: A test of our knowledge of Earth as a system. Science, 290: 291–296
Fransson A, Chierici M, Nojiri Y. 2006. Increased net CO_2 outgassing in the upwelling region of the southern Bering Sea in a period of variable marine climate between 1995 and 2001. J Geophys Res, 111: C08008
Friederich G E, Ledesma J, Ulloa O, Chavez F P. 2008. Air-sea carbon dioxide fluxes in the coastal southeastern tropical Pacific. Prog Oceanogr, 79: 156–166
Friederich G E, Walz P M, Burczynski M G, Chavez F P. 2002. Inorganic carbon in the central California upwelling system during the 1997–1999 El Niño-La Niña event. Prog Oceanogr, 54: 185–203
Gagan M K, Ayliffe L K, Opdyke B N, Hopley D, Scott-Gagan H, Cowley J. 2002. Coral oxygen isotope evidence for recent groundwater fluxes to the Australian Great Barrier Reef. Geophys Res Lett, 29: 43-1–43-4
Gan J, Li H, Curchitser E N, Haidvogel D B. 2006. Modeling South China Sea circulation: Response to seasonal forcing regimes. J Geophys Res, 111: C06034
Gao Z, Chen L, Sun H, Chen B, Cai W J. 2012. Distributions and air-sea fluxes of carbon dioxide in the Western Arctic Ocean. Deep-Sea Res Part II-Top Stud Oceanogr, 81-84: 46–52
Guo X, Cai W J, Zhai W, Dai M, Wang Y, Chen B. 2008. Seasonal variations in the inorganic carbon system in the Pearl River (Zhujiang) estuary. Cont Shelf Res, 28: 1424–1434
Guo X, Dai M, Zhai W, Cai W J, Chen B. 2009. CO_2 flux and seasonal variability in a large subtropical estuarine system, the Pearl River Estuary, China. J Geophys Res, 114: G03013
Guo H Q, Noormets A, Zhao B, Chen J Q, Sun G, Gu Y J, Li B, Chen J K. 2009. Tidal effects on net ecosystem exchange of carbon in an estuarine wetland. Agric For Meteorol, 149: 1820–1828
Guo X H, Zhai W D, Dai M H, Zhang C, Bai Y, Xu Y, Li Q, Wang G Z. 2015. Air-sea CO_2 fluxes in the East China Sea based on multiple-year underway observations. Biogeosciences, 12: 5495–5514
Guo X, Zhang Y, Zhang F, Cao Q. 2010. Characteristics and flux of settling particulate matter in neritic waters: The southern Yellow Sea and the East China Sea. Deep-Sea Res Part II-Top Stud Oceanogr, 57: 1058–1063
Hales B, Takahashi T, Bandstra L. 2005. Atmospheric CO_2 uptake by a coastal upwelling system. Glob Biogeochem Cycle, 19: GB1009
Hopkinson C S, Cai W J, Hu X. 2012. Carbon sequestration in wetland dominated coastal systems—A global sink of rapidly diminishing magnitude. Curr Opin Env Sust, 4: 186–194
Ho T Y, You C F, Chou W C, Pai S C, Wen L S, Sheu D D. 2009. Cadmium and phosphorus cycling in the water column of the South China Sea: The roles of biotic and abiotic particles. Mar Chem, 115: 125–133
Hood E M, Merlivat L, Johannessen T. 1999. Variations of fCO_2 and air-sea flux of CO_2 in the Greenland Sea gyre using high-frequency time series data from CARIOCA drift buoys. J Geophys Res, 104: 20571–

20583
Hu D, Yang Z. 2001. Key Processes of Ocean Fluxes in the East China Sea (in Chinese). Beijing: Ocean Press. 205
Huang T H, Chen C T A, Tseng H C, Lou J Y, Wang S L, Yang L, Kandasamy S, Gao X, Wang J T, Aldrian E, Jacinto G S, Anshari G Z, Sompongchaiyakul P, Wang B J. 2017. Riverine carbon fluxes to the South China Sea. J Geophys Res, 122: 1239–1259
Hung C C, Tseng C W, Gong G C, Chen K S, Chen M H, Hsu S C. 2013. Fluxes of particulate organic carbon in the East China Sea in summer. Biogeosciences, 10: 6469–6484
Ito R G, Schneider B, Thomas H. 2005. Distribution of surface fCO_2 and air-sea fluxes in the Southwestern subtropical Atlantic and adjacent continental shelf. J Mar Syst, 56: 227–242
Jiao N Z, Herndl G J, Hansell D A, Benner R, Kattner G, Wilhelm S W, Kirchman D L, Weinauer M G, Luo T W, Chen F, Azam F. 2010. Microbial production of recalcitrant dissolved organic matter: Long-term carbon storage in the global ocean. Nat Rev Microbiol, 8: 593–599
Kang D J, Kim J Y, Lee T, Kim K R. 2010. The East Sea (Sea of Japan). In: Liu K K, Atkinson L, Quiñones R, Talaue-Mamanus L, eds. Carbon and Nutrient Fluxes in Continental Margins: A global Synthesis. Heidelberg: Springer-Verlag. 383–393
Laruelle G G, Dürr H H, Slomp C P, Borges A V. 2010. Evaluation of sinks and sources of CO_2 in the global coastal ocean using a spatially-explicit typology of estuaries and continental shelves. Geophys Res Lett, 37: L15607
Laruelle G G, Lauerwald R, Pfeil B, Regnier P. 2014. Regionalized global budget of the CO_2 exchange at the air-water interface in continental shelf seas. Glob Biogeochem Cycle, 28: 1199–1214
Le Quéré C, Andrew R M, Friedlingstein P, Sitch S, Pongratz J, Manning A C, Korsbakken J I, Peters G P, Canadell J G, Jackson R B, Boden T A, Tans P P, Andrews O D, Arora V K, Bakker D C E, Barbero L, Becker M, Betts R A, Bopp L, Chevallier F, Chini L P, Ciais P, Cosca C E, Cross J, Currie K, Gasser T, Harris I, Hauck J, Haverd V, Houghton R A, Hunt C W, Hurtt G, Ilyina T, Jain A K, Kato E, Kautz M, Keeling R F, Klein Goldewijk K, Körtzinger A, Landschützer P, Lefèvre N, Lenton A, Lienert S, Lima I, Lombardozzi D, Metzl N, Millero F, Monteiro P M S, Munro D R, Nabel J E M S, Nakaoka S, Nojiri Y, Padín X A, Peregon A, Pfeil B, Pierrot D, Poulter B, Rehder G, Reimer J, Rödenbeck C, Schwinger J, Séférian R, Skjelvan I, Stocker B D, Tian H, Tilbrook B, van der Laan-Luijkx I T, van der Werf G R, van Heuven S, Viovy N, Vuichard N, Walker A P, Watson A J, Wiltshire A J, Zaehle S, Zhu D. 2017. Global carbon budget 2017. Earth Syst Sci Data, 10: 405–448
Li H, Wiesner M G, Chen J, Ling Z, Zhang J, Ran L. 2017. Long-term variation of mesopelagic biogenic flux in the central South China Sea: Impact of monsoonal seasonality and mesoscale eddy. Deep-Sea Res Part I-Oceanogr Res Pap, 126: 62–72
Li L, Qu T D. 2006. Thermohaline circulation in the deep South China Sea basin inferred from oxygen distributions. J Geophys Res, 111: C05017
Liu H, Ren H, Hui D, Wang W, Liao B, Cao Q. 2014. Carbon stocks and potential carbon storage in the mangrove forests of China. J Environ Manage, 133: 86–93
Liu K K, Atkinson L, Quiñones R, Talaue-Mcmanus L. 2010a. Carbon and Nutrient Fluxes in Continental Margins: A Global Synthesis. Heidelberg: Springer. 741
Liu K K, Atkinson L, Quiñones R, Talaue-Mcmanus L. 2010b. Biogeochemistry of the Kuroshio and the East China Sea. In: Liu K K, Atkinson L, Quiñones R, Talaue-Mcmanus L, eds. Carbon and Nutrient Fluxes in Continental Margins: A Global Synthesis. IGBP Book Series. Heidelberg: Springer. 3–24
Liu K K, Chao S Y, Marra J, Snidvongs A. 2006. Monsoonal forcing and biogeochemical environments of outer southeast Asia seas. In: Robinson A, Brink K H, eds. The Sea: Ideas and Observations on Progress in the Study of Seas, the Global Coastal Ocean: Interdisciplinary Regional Studies and Synthesis. Cambridge: Harvard University Press. 673–721
Liu K K, Iseki K, Chao S Y. 2000. Continental margin carbon fluxes. In: Hanson R B, Ducklow H W, Field J G, eds. The Changing Ocean Carbon Cycle. Cambridge: Cambridge University Press. 187–239
Liu Q, Charette M A, Henderson P B, McCorkle D C, Martin W, Dai M. 2014. Effect of submarine groundwater discharge on the coastal ocean inorganic carbon cycle. Limnol Oceanogr, 59: 1529–1554
Liu Q, Dai M, Chen W, Huh C A, Wang G, Li Q, Charette M A. 2012. How significant is submarine groundwater discharge and its associated dissolved inorganic carbon in a river-dominated shelf system? Biogeosciences, 9: 1777–1795
Liu Z, Zhang L, Cai W J, Wang L, Xue M, Zhang X. 2014. Removal of dissolved inorganic carbon in the Yellow River Estuary. Limnol Oceanogr, 59: 413–426
Lu X, Song J, Yuan H, Li N. 2015. Carbon distribution and exchange of Kuroshio and adjacent China sea shelf: A review (in Chinese). Adv Earth Sci, 30: 214–225
Luo X, Wei H, Liu Z, Zhao L. 2015. Seasonal variability of air-sea CO_2 fluxes in the Yellow and East China Seas: A case study of continental shelf sea carbon cycle model. Cont Shelf Res, 107: 69–78
Maher D T, Santos I R, Golsby-Smith L, Gleeson J, Eyre B D. 2013. Groundwater-derived dissolved inorganic and organic carbon exports from a mangrove tidal creek: The missing mangrove carbon sink? Limnol Oceanogr, 58: 475–488
McKee B A. 2003. RiOMar: The Transport, Transformation and Fate of Carbon in River-Dominated Ocean Margins. RiOMar Workshop. Tulane University
Moore W S. 1999. The subterranean estuary: A reaction zone of ground water and sea water. Mar Chem, 65: 111–125
Nakaoka S I, Aoki S, Nakazawa T, Hashida G, Morimoto S, Yamanouchi T, Yoshikawa-Inoue H. 2006. Temporal and spatial variations of oceanic pCO_2 and air-sea CO_2 flux in the Greenland Sea and the Barents Sea. Tellus Ser B-Chem Phys Meteorol, 58: 148–161
Ni H G, Lu F H, Luo X L, Tian H Y, Zeng E Y. 2008. Riverine inputs of total organic carbon and suspended particulate matter from the Pearl River Delta to the coastal ocean off South China. Mar Pollut Bull, 56: 1150–1157
Nozaki Y, Yamamoto Y. 2001. Radium 228 based nitrate fluxes in the eastern Indian Ocean and the South China Sea and a silicon-induced "alkalinity pump" hypothesis. Glob Biogeochem Cycle, 15: 555–567
Oh D C, Park M K, Kim K R. 2000. CO_2 exchange at air-sea interface in the Huanghai Sea. Acta Oceanol Sin, 19: 79–89
Omar A M, Johannessen T, Olsen A, Kaltin S, Rey F. 2007. Seasonal and interannual variability of the air-sea CO_2 flux in the Atlantic sector of the Barents Sea. Mar Chem, 104: 203–213
Pan Y, Birdsey R A, Fang J, Houghton R, Kauppi P E, Kurz W A, Phillips O L, Shvidenko A, Lewis S L, Canadell J G, Ciais P, Jackson R B, Pacala S W, McGuire A D, Piao S, Rautiainen A, Sitch S, Hayes D. 2011. A large and persistent carbon sink in the world's forests. Science, 333: 988–993
Peng T H, Hung J J, Wanninkhof R, Millero F J. 1999. Carbon budget in the East China Sea in spring. Tellus Ser B-Chem Phys Meteorol, 51: 531–540
Qu B X, Song J M, Yuan H M, Li X G, Li N. 2014. Air-sea CO_2 exchange process in the southern Yellow Sea in April of 2011, and June, July, October of 2012. Cont Shelf Res, 80: 8–19
Qu T, Girton J B, Whitehead J A. 2006. Deepwater overflow through Luzon strait. J Geophys Res, 111: C01002
Ran L, Lu X X, Sun H, Han J, Li R, Zhang J. 2013. Spatial and seasonal variability of organic carbon transport in the Yellow River, China. J Hydrol, 498: 76–88
Regnier P, Friedlingstein P, Ciais P, Mackenzie F T, Gruber N, Janssens I A, Laruelle G G, Lauerwald R, Luyssaert S, Andersson A J, Arndt S, Arnosti C, Borges A V, Dale A W, Gallego-Sala A, Goddéris Y, Goossens N, Hartmann J, Heinze C, Ilyina T, Joos F, LaRowe D E, Leifeld J, Meysman F J R, Munhoven G, Raymond P A, Spahni R, Suntharalingam P, Thullner M. 2013. Anthropogenic perturbation of the carbon fluxes from land to ocean. Nat Geosci, 6: 597–607
Rehder G, Suess E. 2001. Methane and pCO_2 in the Kuroshio and the South

China Sea during maximum summer surface temperatures. Mar Chem, 75: 89–108
Sabine C L, Feely R A, Gruber N, Key R M, Lee K, Bullister J L, Wanninkhof R, Wong C S, Wallace D W R, Tilbrook B, Millero F J, Peng T H, Kozyr A, Ono T, Rios A F. 2004. The oceanic sink for anthropogenic CO_2. Science, 305: 367–371
Sadat-Noori M, Maher D T, Santos I R. 2016. Groundwater discharge as a source of dissolved carbon and greenhouse gases in a subtropical estuary. Estuaries Coasts, 39: 639–656
Sanders C J, Maher D T, Tait D R, Williams D, Holloway C, Sippo J Z, Santos I R. 2016. Are global mangrove carbon stocks driven by rainfall? J Geophys Res, 121: 2600–2609
Santos I R, Burnett W C, Dittmar T, Suryaputra I G N A, Chanton J. 2009. Tidal pumping drives nutrient and dissolved organic matter dynamics in a gulf of mexico subterranean estuary. Geochim Cosmochim Acta, 73: 1325–1339
Sarmiento J L, Gruber N. 2002. Sinks for anthropogenic carbon. Phys Today, 55: 30–36
Semiletov I P, Pipko I I, Repina I, Shakhova N E. 2007. Carbonate chemistry dynamics and carbon dioxide fluxes across the atmosphere-ice-water interfaces in the Arctic Ocean: Pacific sector of the Arctic. J Mar Syst, 66: 204–226
Sheu D D, Chou W C, Chen C T A, Wei C L, Hsieh H L, Hou W P, Dai M. 2009. Riding over the Kuroshio from the South to the East China Sea: Mixing and transport of DIC. Geophys Res Lett, 36: L07603
Sheu D D, Chou W C, Wei C L, Hou W P, Wong G T F, Hsu C W. 2010. Influence of El Niño on the sea-to-air CO_2 flux at the SEATS time-series site, northern South China Sea. J Geophys Res, 115: C10021
Shim J H, Kim D, Kang Y C, Lee J H, Jang S T, Kim C H. 2007. Seasonal variations in pCO_2 and its controlling factors in surface seawater of the northern East China Sea. Cont Shelf Res, 27: 2623–2636
Sippo J Z, Maher D T, Tait D R, Ruiz-Halpern S, Sanders C J, Santos I R. 2017. Mangrove outwelling is a significant source of oceanic exchangeable organic carbon. Limnol Oceanogr, 2: 1–8
Skjelvan I, Johannessen T, Miller L A. 1999. Interannual variability of fCO_2 in the Greenland and Norwegian Seas. Tellus Ser B-Chem Phys Meteorol, 51: 477–489
Slagstad D, Downing K, Carlotti F, Hirche H J. 1999. Modelling the carbon export and air-sea flux of CO_2 in the Greenland Sea. Deep-Sea Res Part II-Top Stud Oceanogr, 46: 1511–1530
Søvik A K, Kløve B. 2007. Emission of N_2O and CH_4 from a constructed wetland in southeastern Norway. Sci Total Environ, 380: 28–37
Sutula M A, Perez B C, Reyes E, Childers D L, Davis S, Day Jr. J W, Rudnick D, Sklar F. 2003. Factors affecting spatial and temporal variability in material exchange between the Southern Everglades wetlands and Florida Bay (USA). Estuar Coast Shelf Sci, 57: 757–781
State Oceanic Administration. 2013. China's Marine Environment Bulletin in 2012 (in Chinese). 75–77
Takahashi T, Sutherland S C, Wanninkhof R, Sweeney C, Feely R A, Chipman D W, Hales B, Friederich G, Chavez F, Sabine C, Watson A, Bakker D C E, Schuster U, Metzl N, Yoshikawa-Inoue H, Ishii M, Midorikawa T, Nojiri Y, Körtzinger A, Steinhoff T, Hoppema M, Olafsson J, Arnarson T S, Tilbrook B, Johannessen T, Olsen A, Bellerby R, Wong C S, Delille B, Bates N R, de Baar H J W. 2009. Climatological mean and decadal change in surface ocean pCO_2, and net sea-air CO_2 flux over the global oceans. Deep-Sea Res Part II-Top Stud Oceanogr, 56: 554–577
Thomas H, Schneider B. 1999. The seasonal cycle of carbon dioxide in Baltic Sea surface waters. J Mar Syst, 22: 53–67
Thomas H, Bozec Y, de Baar H J W, Elkalay K, Frankignoulle M, Schiettecatte L S, Kattner G, Borges A V. 2005. The carbon budget of the North Sea. Biogeosciences, 2: 87–96
Thomas H, Bozec Y, Elkalay K, de Baar H J W. 2004. Enhanced open ocean storage of CO_2 from shelf sea pumping. Science, 304: 1005–1008
Tian J W, Yang Q X, Liang X F, Xie L L, Hu D X, Wang F, Qu T D. 2006. Observation of Luzon Strait transport. Geophys Res Lett, 33: L19607
Torres R, Turner D R, Rutllant J, Lefèvre N. 2003. Continued CO_2 outgassing in an upwelling area off northern Chile during the development phase of El Niño 1997–1998 (July 1997). J Geophys Res, 108: 3336
Torres R, Pantoja S, Harada N, González H E, Daneri G, Frangopulos M, Rutllant J A, Duarte C M, Rúiz-Halpern S, Mayol E, Fukasawa M. 2011. Air-sea CO_2 fluxes along the coast of Chile: From CO_2 outgassing in central northern upwelling waters to CO_2 uptake in southern Patagonian fjords. J Geophys Res, 116: C09006
Tseng C M, Liu K K, Gong G C, Shen P Y, Cai W J. 2011. CO_2 uptake in the East China Sea relying on Changjiang runoff is prone to change. Geophys Res Lett, 38: L24609
Tseng C M, Shen P Y, Liu K K. 2014. Synthesis of observed air-sea CO_2 exchange fluxes in the river-dominated East China Sea and improved estimates of annual and seasonal net mean fluxes. Biogeosciences, 11: 3855–3870
Tseng C M, Wong G T F, Chou W C, Lee B S, Sheu D D, Liu K K. 2007. Temporal variations in the carbonate system in the upper layer at the SEATS station. Deep-Sea Res Part II-Top Stud Oceanogr, 54: 1448–1468
Tsunogai S, Watanabe S, Sato T. 1999. Is there a "continental shelf pump" for the absorption of atmospheric CO_2? Tellus Ser B-Chem Phys Meteorol, 51: 701–712
Vandemark D, Salisbury J E, Hunt C W, Shellito S M, Irish J D, McGillis W R, Sabine C L, Maenner S M. 2011. Temporal and spatial dynamics of CO_2 air-sea flux in the Gulf of Maine. J Geophys Res, 116: C01012
Wang G, Dai M, Shen S S P, Bai Y, Xu Y. 2014. Quantifying uncertainty sources in the gridded data of sea surface CO_2 partial pressure. J Geophys Res, 119: 5181–5189
Wang H, Dai M, Liu J, Kao S J, Zhang C, Cai W J, Wang G, Qian W, Zhao M, Sun Z. 2016. Eutrophication-driven hypoxia in the East China Sea off the Changjiang Estuary. Environ Sci Technol, 50: 2255–2263
Wang G, Wang Z, Zhai W, Moore W S, Li Q, Yan X, Qi D, Jiang Y. 2015. Net subterranean estuarine export fluxes of dissolved inorganic C, N, P, Si, and total alkalinity into the Jiulong River estuary, China. Geochim Cosmochim Acta, 149: 103–114
Wang S L, Arthur Chen C T, Hong G H, Chung C S. 2000. Carbon dioxide and related parameters in the East China Sea. Cont Shelf Res, 20: 525–544
Wang X, Ma H, Li R, Song Z, Wu J. 2012. Seasonal fluxes and source variation of organic carbon transported by two major Chinese Rivers: The Yellow River and Changjiang (Yangtze) River. Glob Biogeochem Cycle, 26: GB2025
Wei C L, Lin S Y, Sheu D D D, Chou W C, Yi M C, Santschi P H, Wen L S. 2011. Particle-reactive radionuclides (^{234}Th, ^{210}Pb, ^{210}Po) as tracers for the estimation of export production in the South China Sea. Biogeosciences, 8: 3793–3808
Wu K, Dai M, Chen J, Meng F, Li X, Liu Z, Du C, Gan J. 2015. Dissolved organic carbon in the South China Sea and its exchange with the Western Pacific Ocean. Deep-Sea Res Part II-Top Stud Oceanogr, 122: 41–51
Wu Y, Zhang J, Liu S M, Zhang Z F, Yao Q Z, Hong G H, Cooper L. 2007. Sources and distribution of carbon within the Yangtze River system. Estuar Coast Shelf Sci, 71: 13–25
Xia B, Zhang L. 2011. Carbon distribution and fluxes of 16 rivers discharging into the Bohai Sea in summer. Acta Oceanol Sin, 30: 43–54
Xu X, Zang K, Zhao H, Zheng N, Huo C, Wang J. 2016. Monthly CO_2 at A4HDYD station in a productive shallow marginal sea (Yellow Sea) with a seasonal thermocline: Controlling processes. J Mar Syst, 159: 89–99
Xue L, Xue M, Zhang L, Sun T, Guo Z, Wang J. 2012. Surface partial pressure of CO_2 and air-sea exchange in the northern Yellow Sea. J Mar Syst, 105-108: 194–206
Xue L, Zhang L, Cai W J, Jiang L Q. 2011. Air-sea CO_2 fluxes in the southern Yellow Sea: An examination of the continental shelf pump hypothesis. Cont Shelf Res, 31: 1904–1914
Yang W F, Huang Y P, Chen M, Qiu Y S, Peng A G, Zhang L. 2009. Export and remineralization of POM in the Southern Ocean and the South China Sea estimated from $^{210}Po/^{210}Pb$ disequilibria. Chin Sci

Bull, 54: 2118–2123
Yin W, Qi Y, Cao Z, Zhang Y, Tang H. 2012. The environmental characteristics of the major Greenhouse gases and seawater pCO_2 in the Bohai Sea (in Chinese). Trans Oceanol Limnol, 4: 189–193
Zhai W D, Dai M. 2009. On the seasonal variation of air-sea CO_2 fluxes in the outer Changjiang (Yangtze River) Estuary, East China Sea. Mar Chem, 117: 2–10
Zhai W D, Dai M, Cai W J. 2009. Coupling of surface pCO_2 and dissolved oxygen in the northern South China Sea: impacts of contrasting coastal processes. Biogeosciences, 6: 2589–2598
Zhai W D, Dai M, Cai W J, Wang Y, Hong H. 2005. The partial pressure of carbon dioxide and air-sea fluxes in the northern South China Sea in spring, summer and autumn. Mar Chem, 96: 87–97
Zhai W D, Dai M H, Chen B S, Guo X H, Li Q, Shang S L, Zhang C Y, Cai W J, Wang D X. 2013. Seasonal variations of sea-air CO_2 fluxes in the largest tropical marginal sea (South China Sea) based on multiple-year underway measurements. Biogeosciences, 10: 7775–7791
Zhai W D, Dai M, Guo X H. 2007. Carbonate system and CO_2 degassing fluxes in the inner estuary of Changjiang (Yangtze) River, China. Mar Chem, 107: 342–356
Zhai W D, Yan X L, Qi D. 2017. Biogeochemical generation of dissolved inorganic carbon and nitrogen in the North Branch of inner Changjiang Estuary in a dry season. Estuar Coast Shelf Sci, 197: 136–149
Zhang F, Liu A, Li Y, Zhao L, Wang Q, Du M. 2008. CO_2 flux in alpine wetland ecosystem on the Qinghai-Tibetan Plateau, China. Acta Ecol Sin, 28: 453–462
Zhang X, Zhang L. 2007. Phenomena of pH instant increasing and its effect on dissolved inorganic carbon flux to sea in Yellow River estuary (in Chinese). Environ Sci, 28: 1216–1222
Zhang Y, Zhang F, Guo X, Zhang M. 2004. Vertical flux of the settling particulate matter in the water column of the Yellow Sea in Summer (in Chinese). Oceanol Limnol Sin, 35: 230–238
Zhang Y, Zhang F, Guo X, Zhang M. 2005. Autumn vertical flux of settling particulate matter at three typical stations in the Yellow Sea (in Chinese). Geochimica, 34: 123–128
Zhou K. 2009. Preliminary research on the distribution, export and dynamics of particulate organic carbon in spring in Yellow Sea. Master Thesis (in Chinese). Xiamen: Xiamen University

(Responsible editor: Chuanlun ZHANG)